RG-K $K^+\Lambda$ Monte Carlo Analysis Pass-1 vs. Pass-2 Reconstruction

D.S. Carman – November 21, 2022

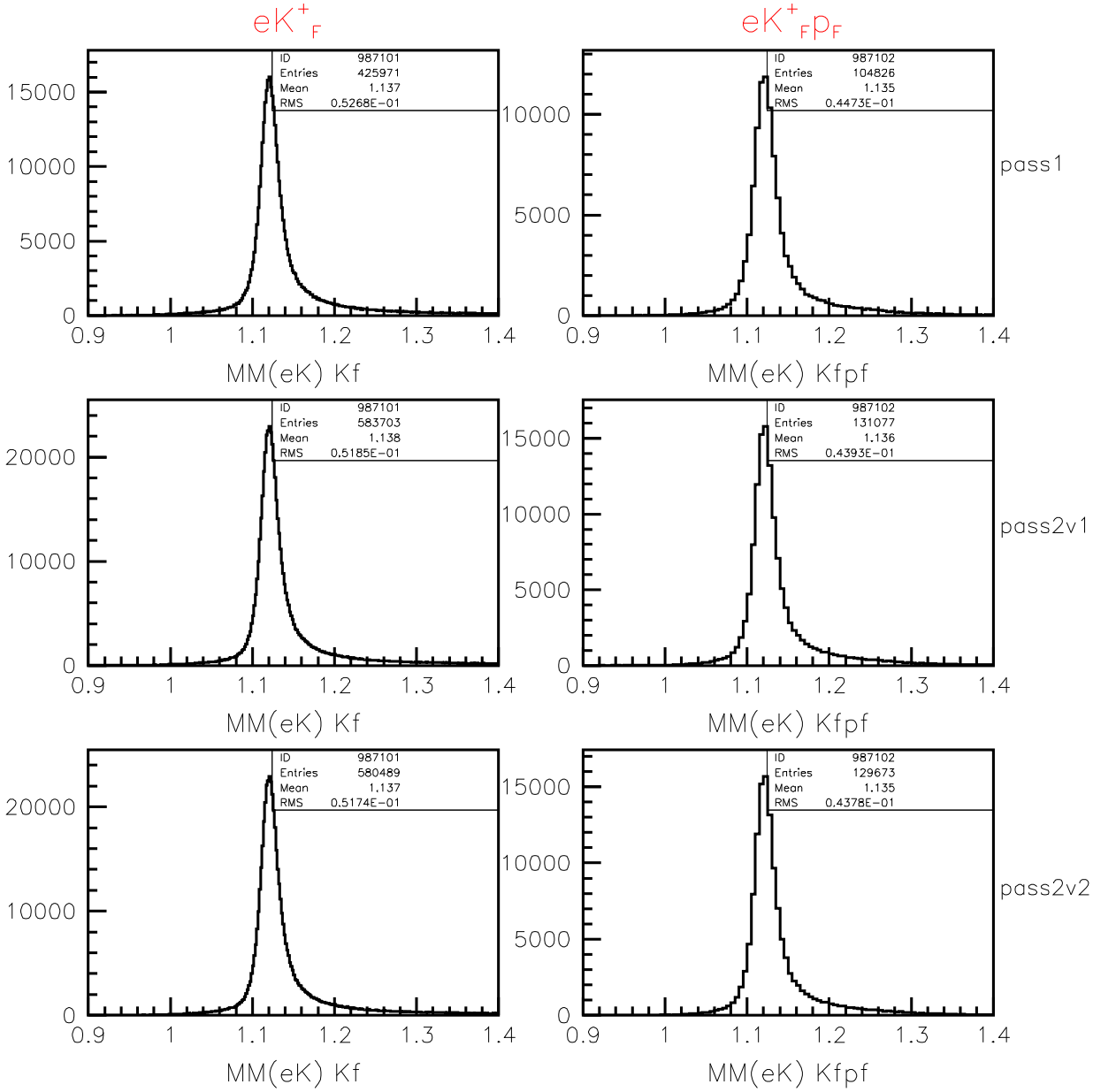

Figure 1: $MM(e'K^+)$ spectra from the RG-K $K^+\Lambda$ Monte Carlo (with background) for E_b=6.535 GeV (outbending torus polarity) comparing the pass-1 reconstruction results (6.5.6.2) to the pass-2 reconstruction results (pass-2 v1 - 8.3.2, pass-2 v2 - 8c.3.2). The electron is reconstructed in the ECAL and the K^+ in the FD. The right plots also require a proton in the FD with a cut on the $MM^2(e'K^+p)$ distribution to select the ground state hyperons.

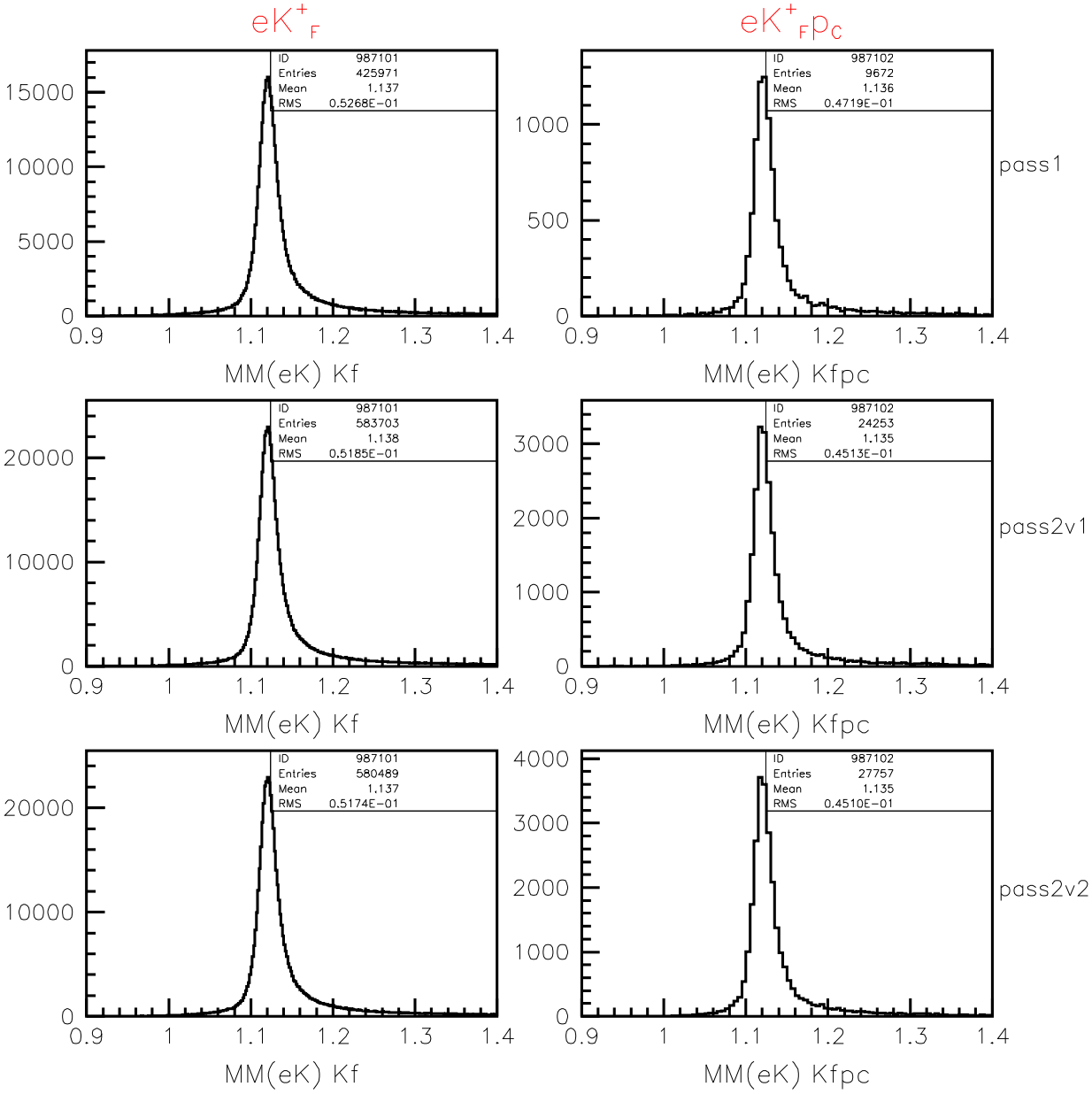

Figure 2: $MM(e'K^+)$ spectra from the RG-K $K^+\Lambda$ Monte Carlo (with background) for E_b=6.535 GeV (outbending torus polarity) comparing the pass-1 reconstruction results (6.5.6.2) to the pass-2 reconstruction results (pass-2 v1 - 8.3.2, pass-2 v2 - 8c.3.2). The electron is reconstructed in the ECAL and the K^+ in the FD. The right plots also require a proton in the CD with a cut on the $MM^2(e'K^+p)$ distribution to select the ground state hyperons.

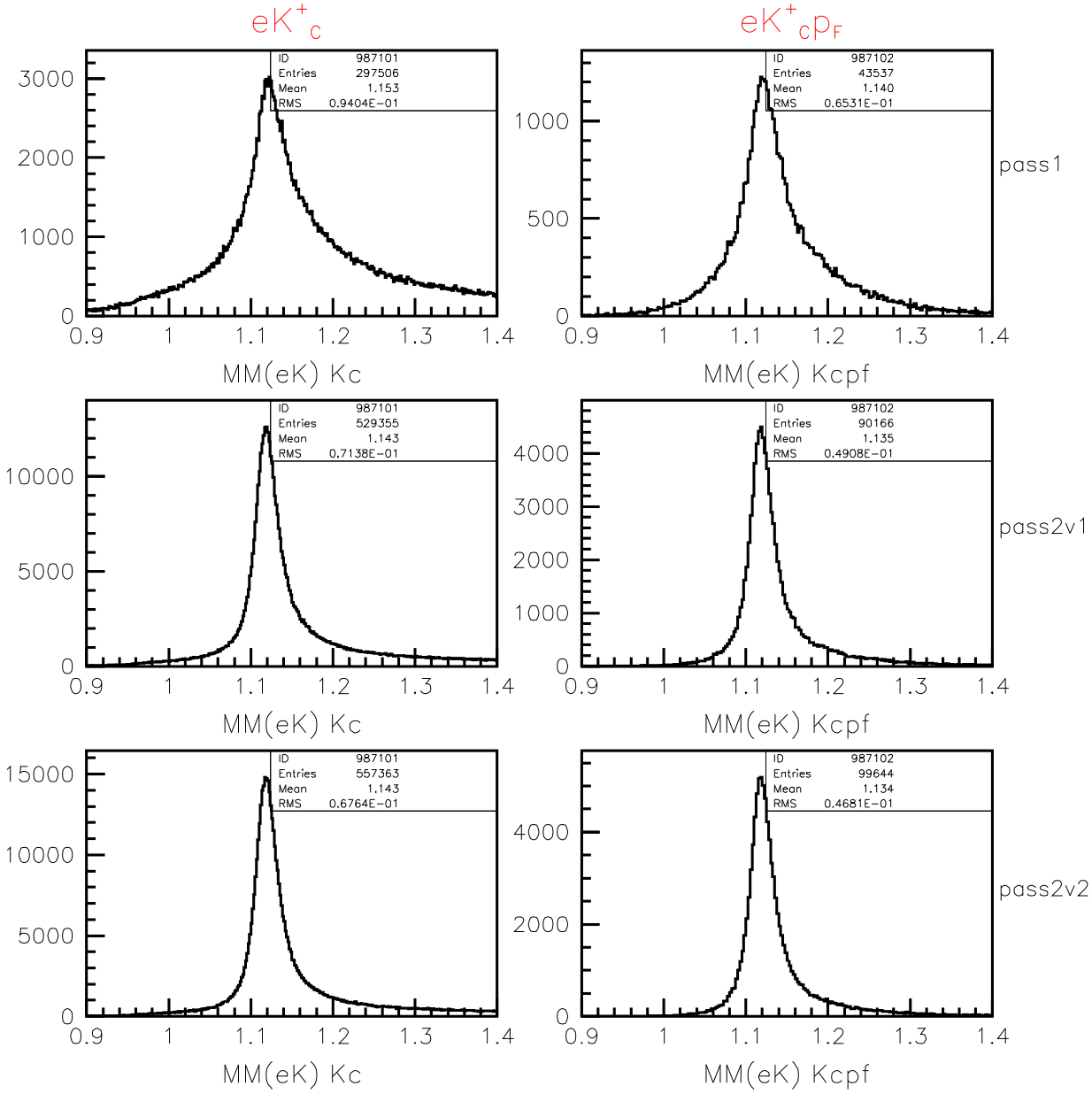

Figure 3: $MM(e'K^+)$ spectra from the RG-K $K^+\Lambda$ Monte Carlo (with background) for E_b=6.535 GeV (outbending torus polarity) comparing the pass-1 reconstruction results (6.5.6.2) to the pass-2 reconstruction results (pass-2 v1 - 8.3.2, pass-2 v2 - 8c.3.2). The electron is reconstructed in the ECAL and the K^+ in the CD. The right plots also require a proton in the FD with a cut on the $MM^2(e'K^+p)$ distribution to select the ground state hyperons.

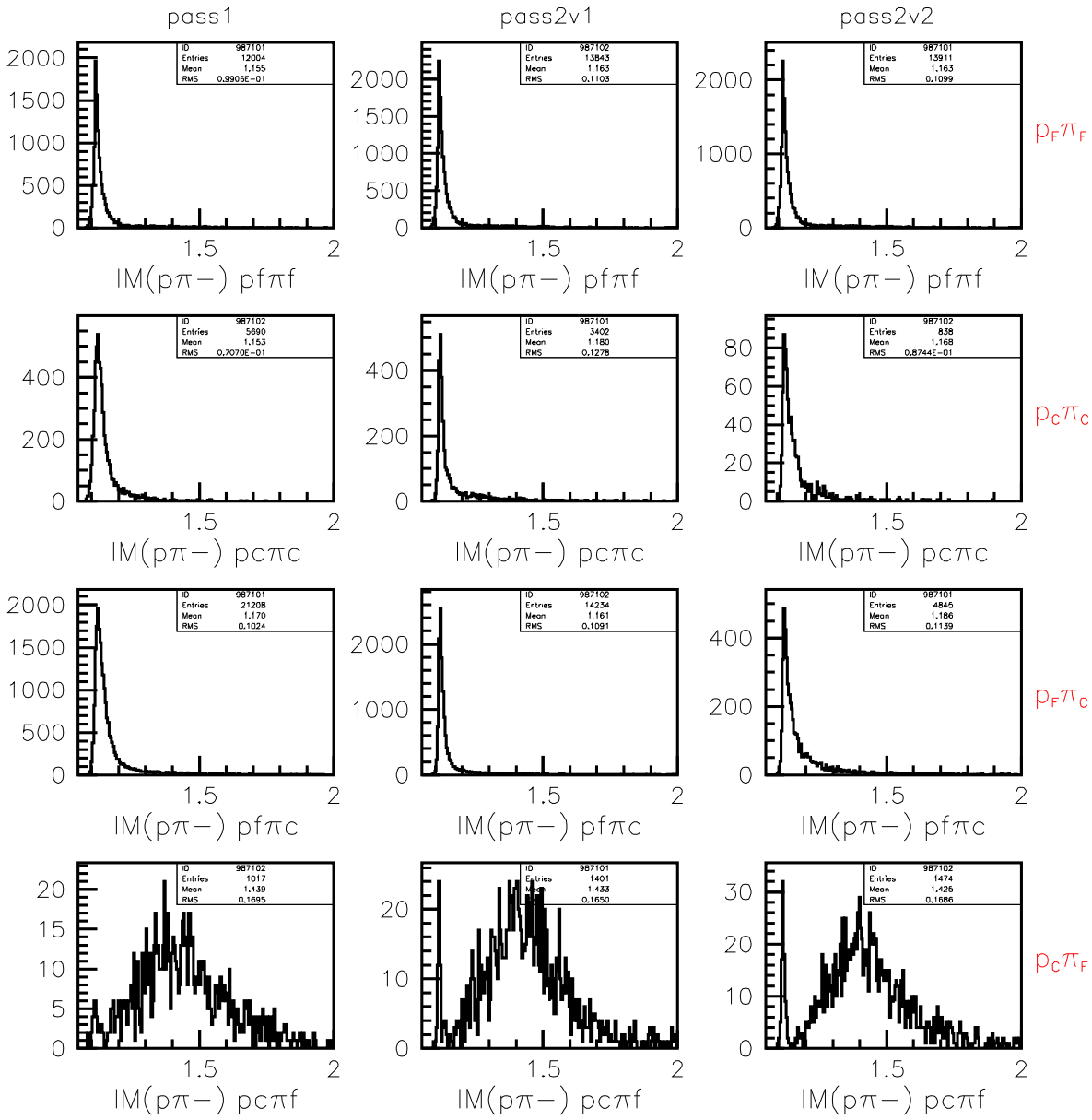

Figure 4: $M(p\pi^-)$ invariant mass spectra from the RG-K $K^+\Lambda$ Monte Carlo (with background) for E_b=6.535 GeV (outbending torus polarity) comparing the pass-1 reconstruction results (6.5.6.2) to the pass-2 reconstruction results (pass-2 v1 - 8.3.2, pass-2 v2 - 8c.3.2). The electron is reconstructed in the ECAL. The different rows are for the different FD/CD p and π^- topologies as labeled.

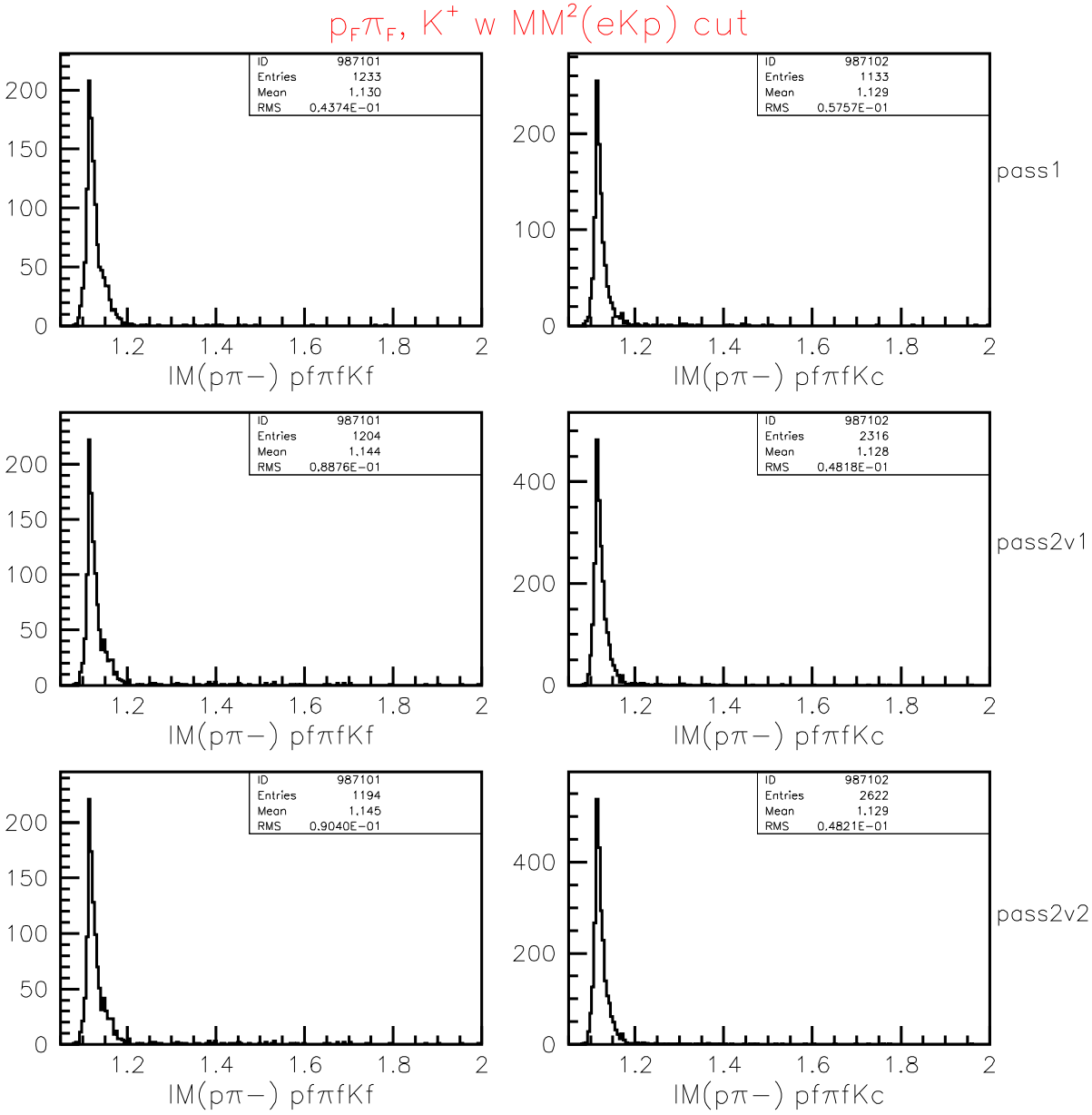

Figure 5: $M(p\pi^-)$ invariant mass spectra from the RG-K $K^+\Lambda$ Monte Carlo (with background) for E_b=6.535 GeV (outbending torus polarity) comparing the pass-1 reconstruction results (6.5.6.2) to the pass-2 reconstruction results (pass-2 v1 - 8.3.2, pass-2 v2 - 8c.3.2). The electron is reconstructed in the ECAL. The plots show the sort for the p FD, π^- FD topology with the requirement of a K^+ in the FD (left) or CD (right). The plots also include a cut on the $MM^2(e'K^+p)$ distribution to select the ground state hyperons.

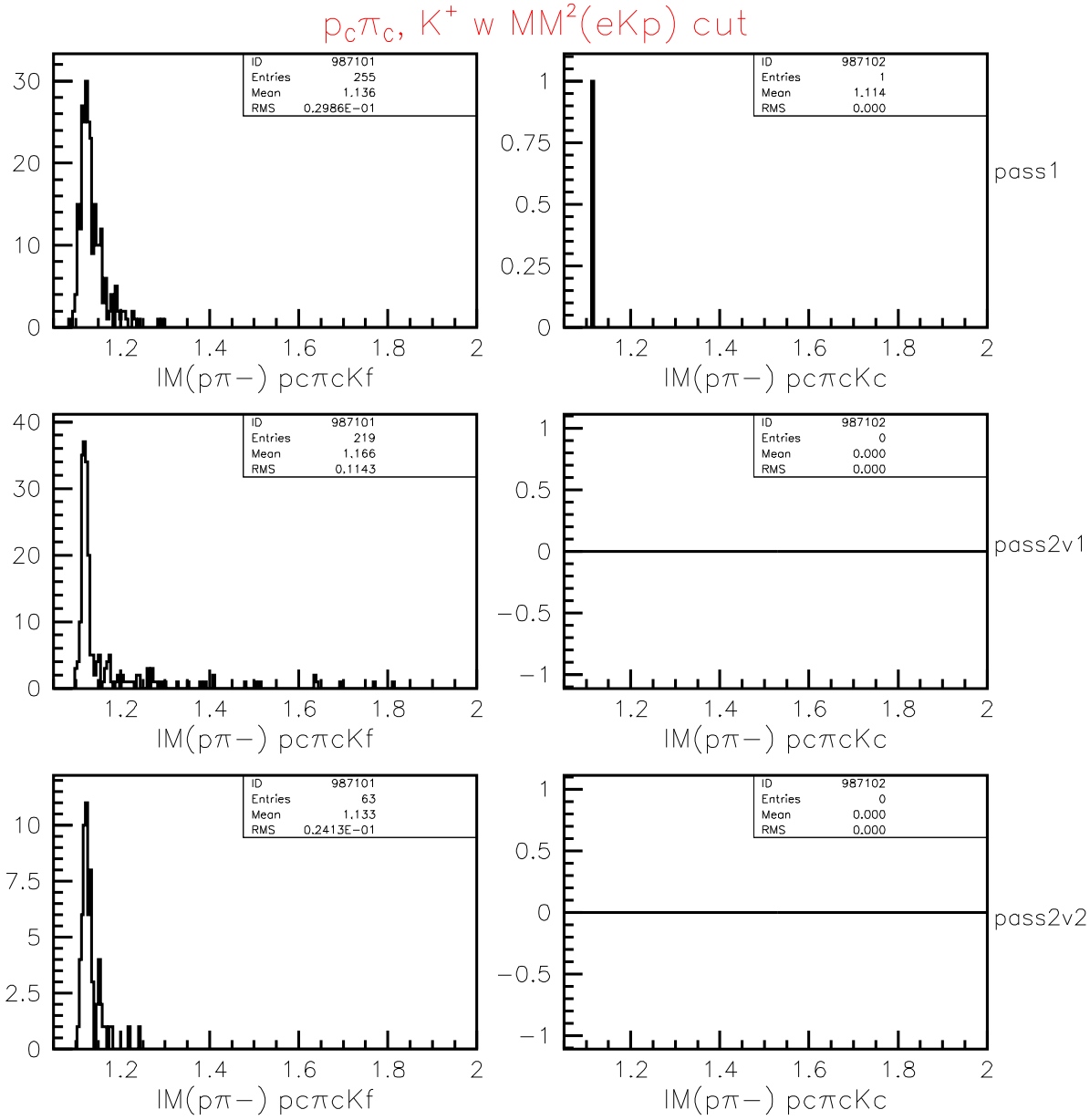

Figure 6: $M(p\pi^-)$ invariant mass spectra from the RG-K $K^+\Lambda$ Monte Carlo (with background) for E_b=6.535 GeV (outbending torus polarity) comparing the pass-1 reconstruction results (6.5.6.2) to the pass-2 reconstruction results (pass-2 v1 - 8.3.2, pass-2 v2 - 8c.3.2). The electron is reconstructed in the ECAL. The plots show the sort for the p CD, π^- CD topology with the requirement of a K^+ in the FD (left) or CD (right). The plots also include a cut on the $MM^2(e'K^+p)$ distribution to select the ground state hyperons.

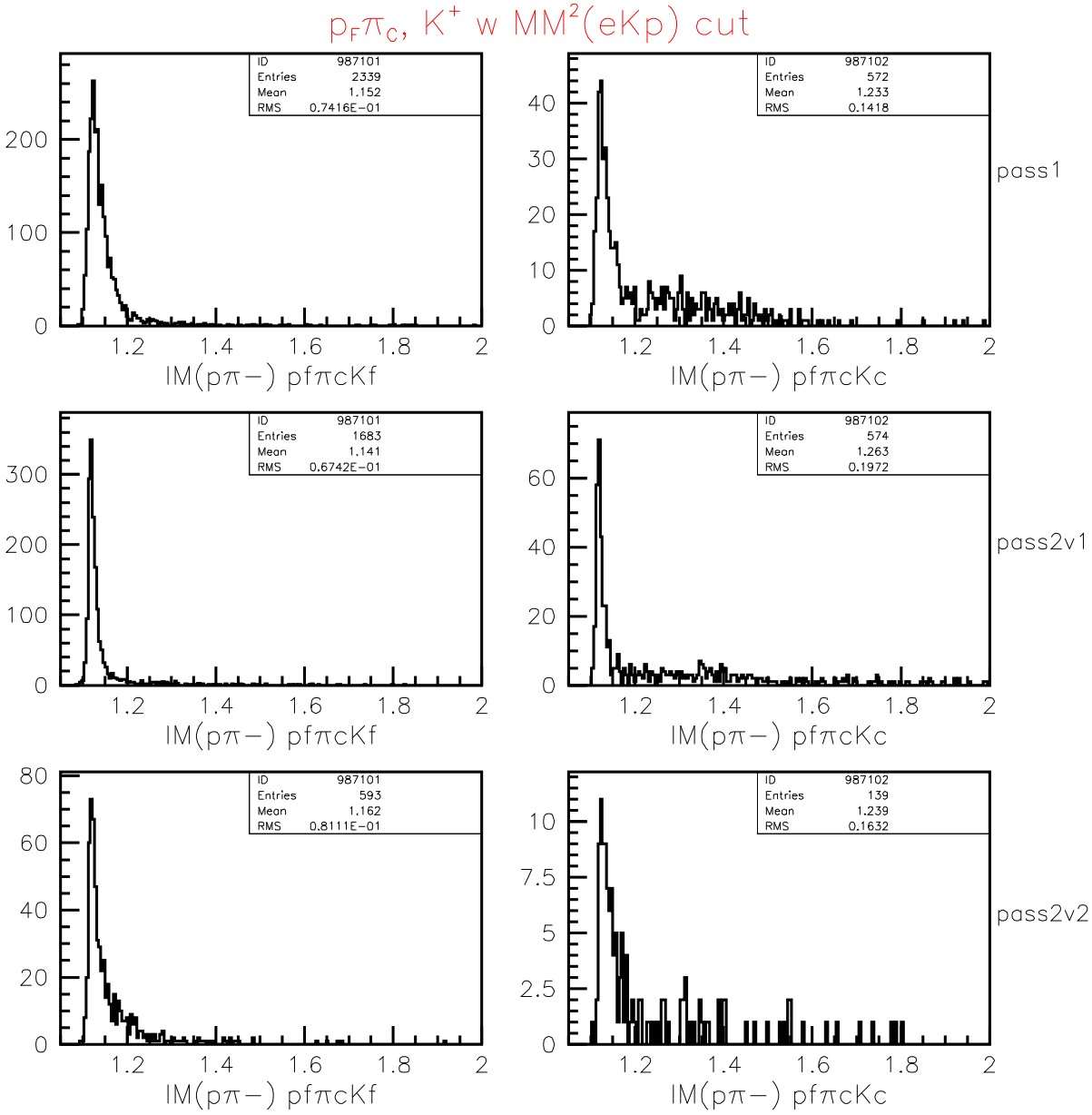

Figure 7: $M(p\pi^-)$ invariant mass spectra from the RG-K $K^+\Lambda$ Monte Carlo (with background) for E_b=6.535 GeV (outbending torus polarity) comparing the pass-1 reconstruction results (6.5.6.2) to the pass-2 reconstruction results (pass-2 v1 - 8.3.2, pass-2 v2 - 8c.3.2). The electron is reconstructed in the ECAL. The plots show the sort for the p FD, π^- CD topology with the requirement of a K^+ in the FD (left) or CD (right). The plots also include a cut on the $MM^2(e'K^+p)$ distribution to select the ground state hyperons.

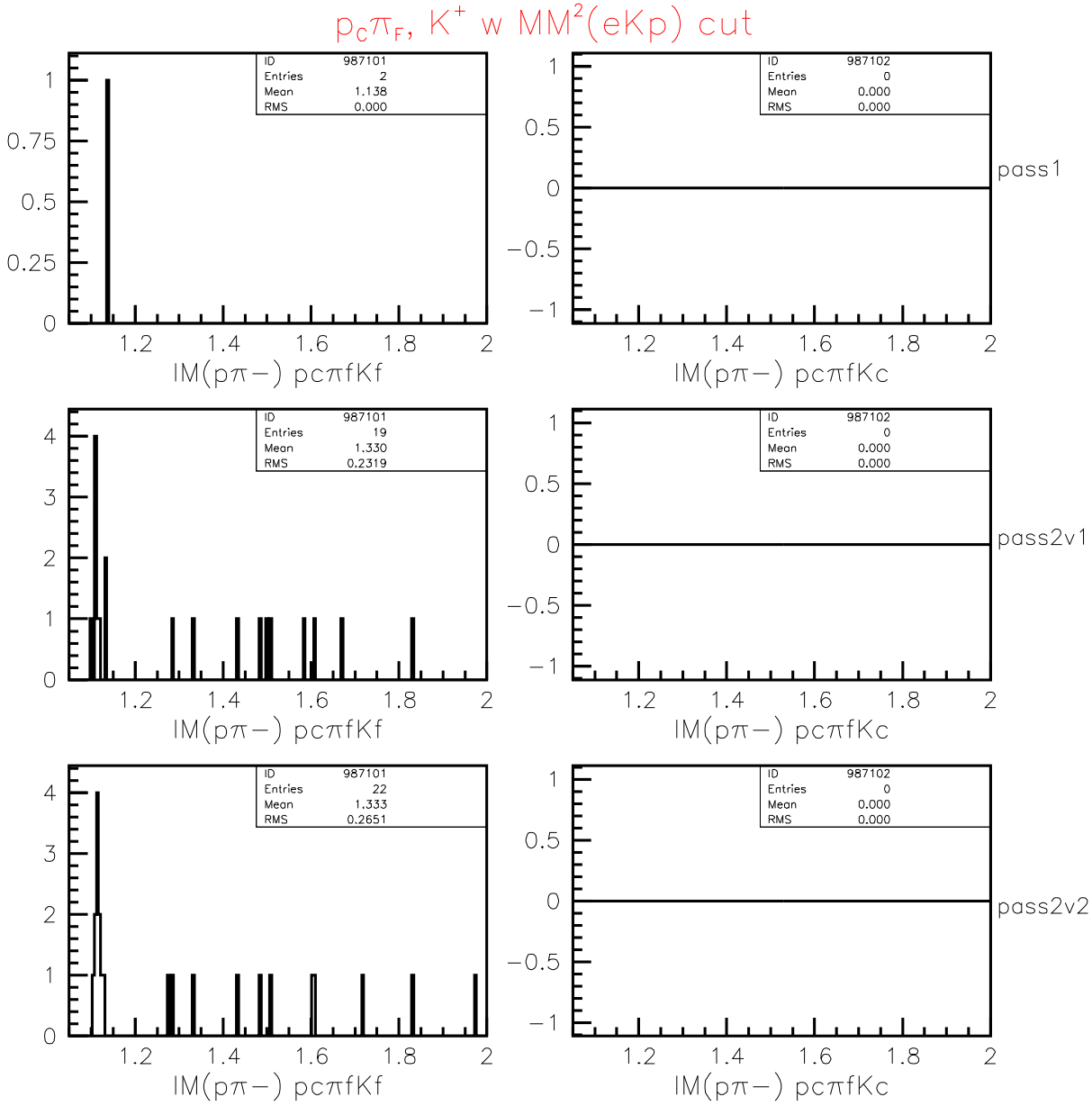

Figure 8: $M(p\pi^-)$ invariant mass spectra from the RG-K $K^+\Lambda$ Monte Carlo (with background) for E_b=6.535 GeV (outbending torus polarity) comparing the pass-1 reconstruction results (6.5.6.2) to the pass-2 reconstruction results (pass-2 v1 - 8.3.2, pass-2 v2 8c.3.2). The electron is reconstructed in the ECAL. The plots show the sort for the p CD, π^- FD topology with the requirement of a K^+ in the FD (left) or CD (right). The plots also include a cut on the $MM^2(e'K^+p)$ distribution to select the ground state hyperons.

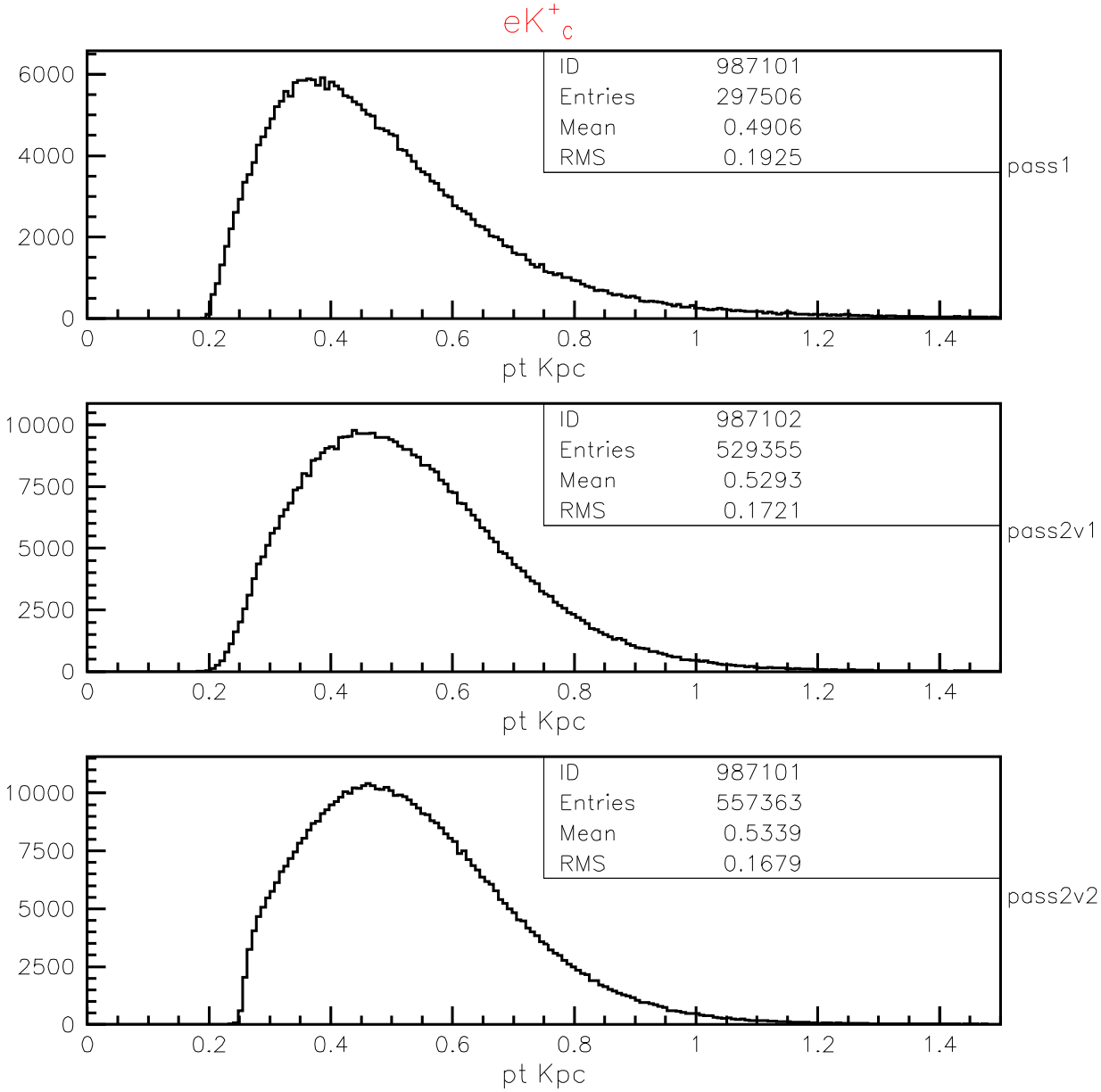

Figure 9: Transverse K^+ momentum spectra from the RG-K $K^+\Lambda$ Monte Carlo (with background) for E_b=6.535 GeV (outbending torus polarity) comparing the pass-1 reconstruction results (6.5.6.2) to the pass-2 reconstruction results (pass-2 v1 - 8.3.2, pass-2 v2 8c.3.2). The electron is reconstructed in the ECAL and the K^+ in the CD.

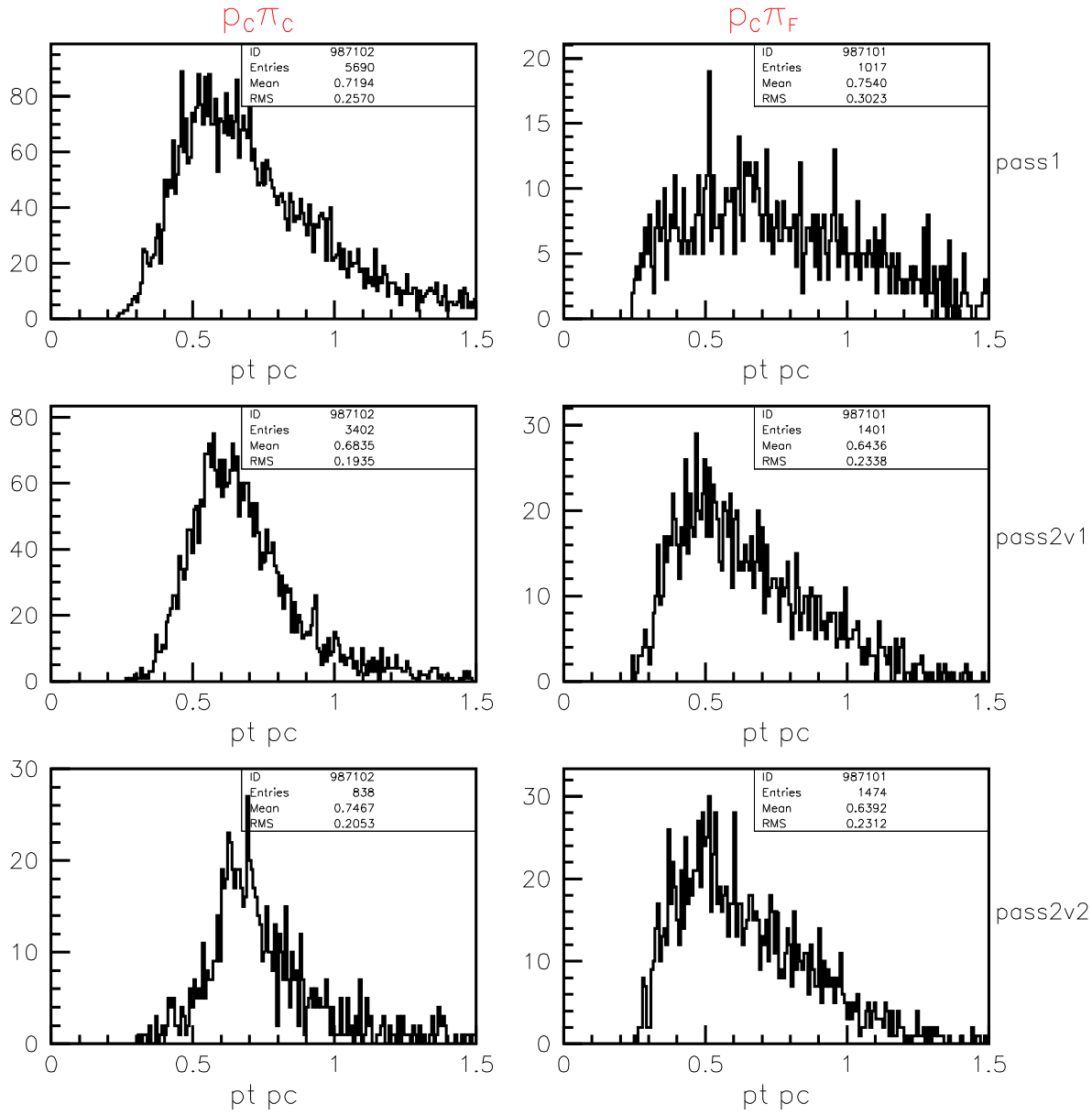

Figure 10: Transverse p momentum spectra from the RG-K $K^+\Lambda$ Monte Carlo (with background) for E_b=6.535 GeV (outbending torus polarity) comparing the pass-1 reconstruction results (6.5.6.2) to the pass-2 reconstruction results (pass-2 v1 - 8.3.2, pass-2 v2 8c.3.2). The electron is reconstructed in the ECAL and the p in the CD. The plots show the sort for the π^- CD (left) and π^- FD (right) topologies.

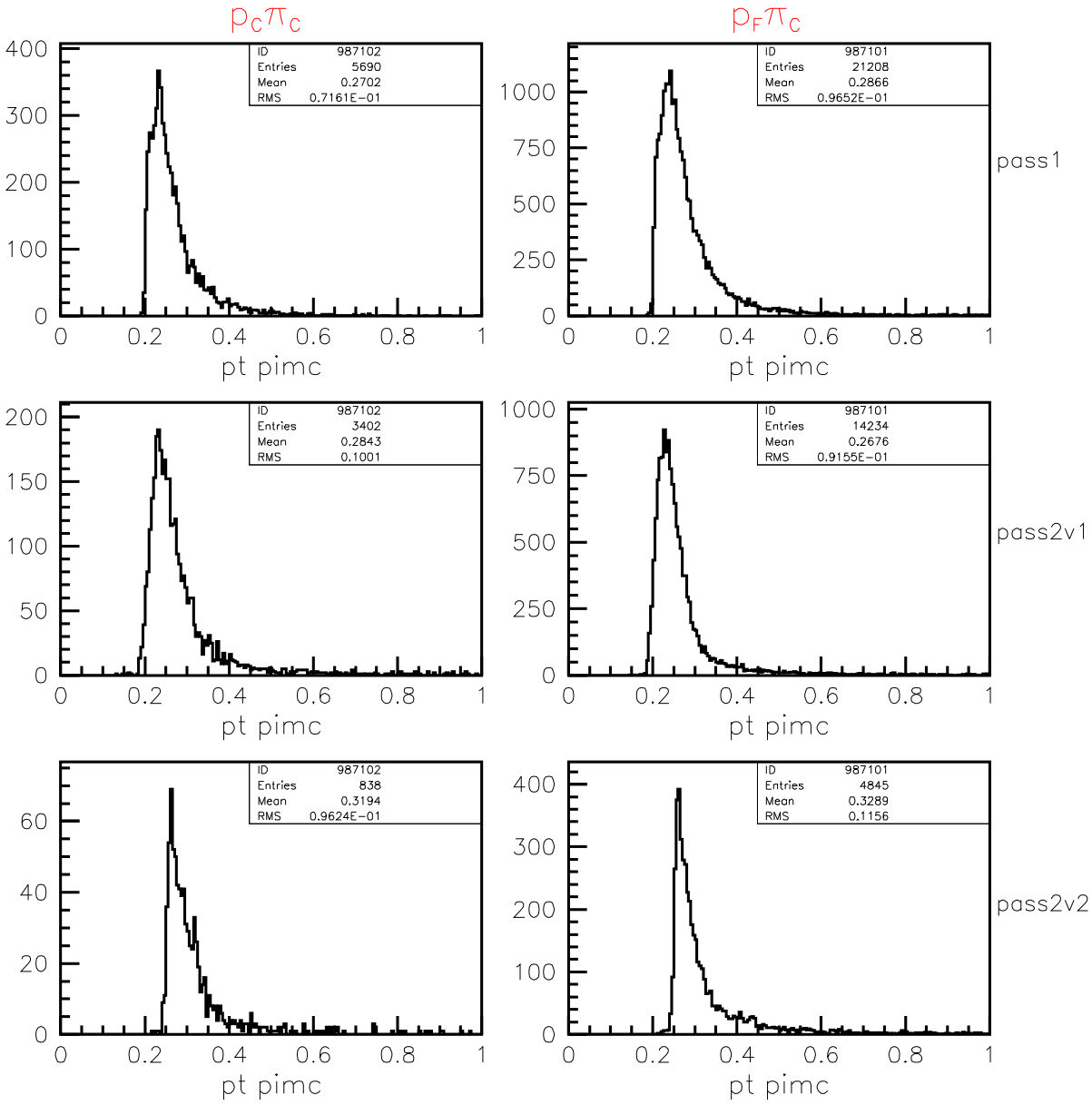

Figure 11: Transverse π^- momentum spectra from the RG-K $K^+\Lambda$ Monte Carlo (with background) for E_b=6.535 GeV (outbending torus polarity) comparing the pass-1 reconstruction results (6.5.6.2) to the pass-2 reconstruction results (pass-2 v1 - 8.3.2, pass-2 v2 8c.3.2). The electron is reconstructed in the ECAL and the π^- in the CD. The plots show the sort for the p CD (left) and p FD (right) topologies.

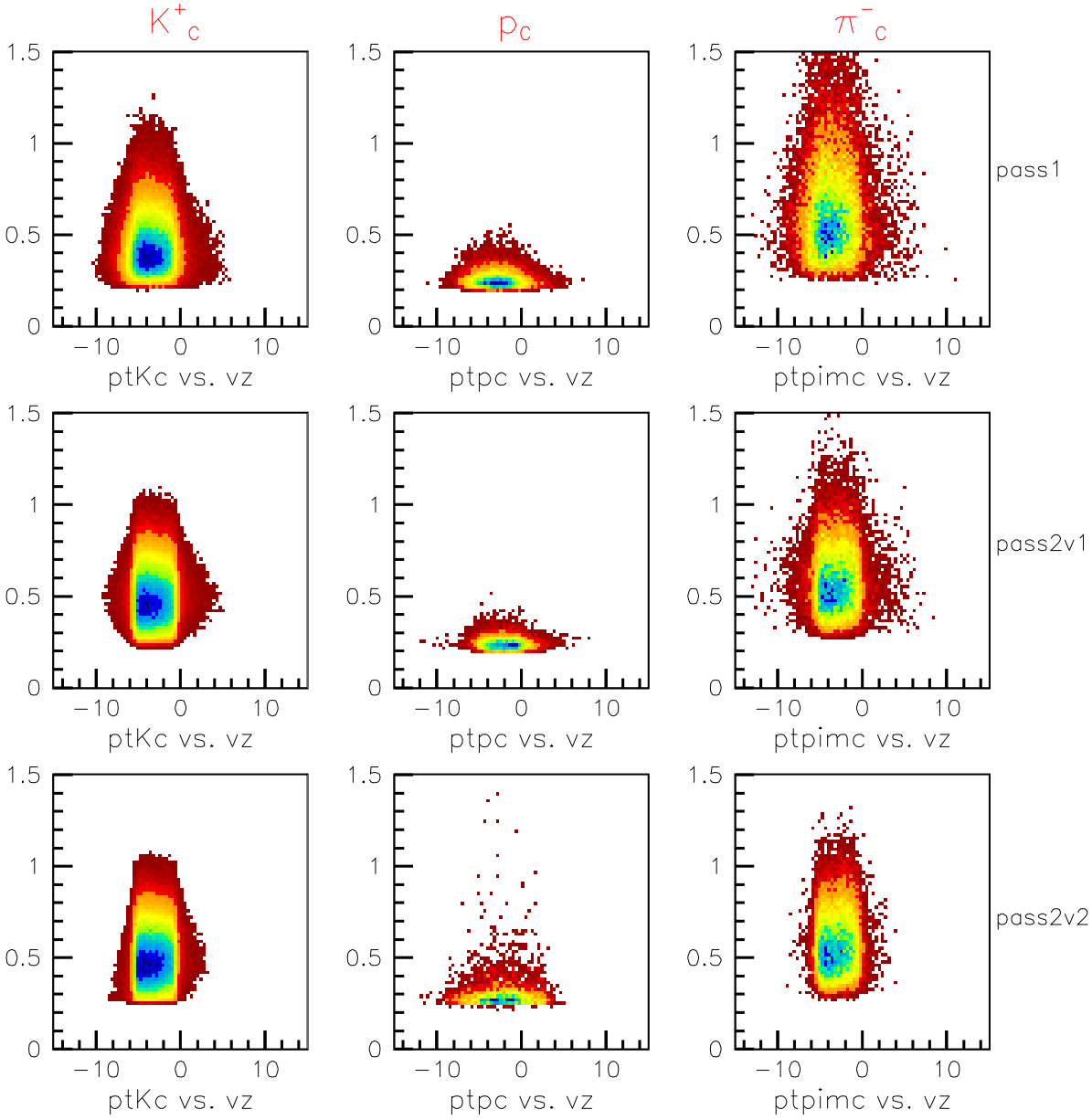

Figure 12: Transverse hadron momentum vs. v_z from the RG-K $K^+\Lambda$ Monte Carlo (with background) for E_b=6.535 GeV (outbending torus polarity) comparing the pass-1 reconstruction results (6.5.6.2) to the pass-2 reconstruction results (pass-2 v1 - 8.3.2, pass-2 v2 8c.3.2). The electron is reconstructed in the ECAL and the hadrons K^+ (left), p (middle), and π^- (right) in the CD.

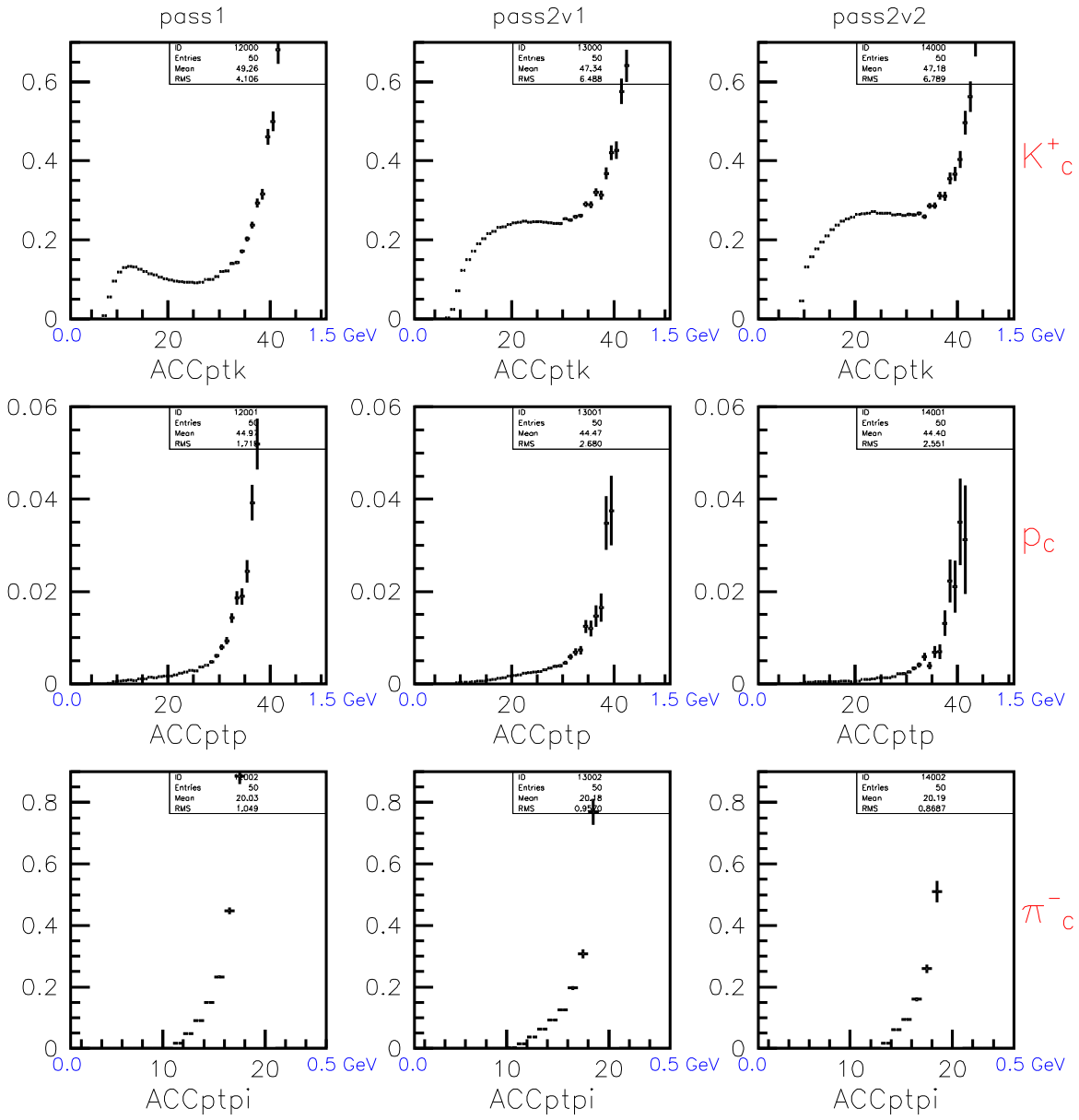

Figure 13: Hadron acceptance vs. transverse hadron momentum from the RG-K $K^+\Lambda$ Monte Carlo (with background) for E_b=6.535 GeV (outbending torus polarity) comparing the pass-1 reconstruction results (6.5.6.2) to the pass-2 reconstruction results (pass-2 v1 - 8.3.2, pass-2 v2 8c.3.2). The electron is reconstructed in the ECAL and the hadrons K^+ (top), p (middle), and π^- (bottom) in the CD.

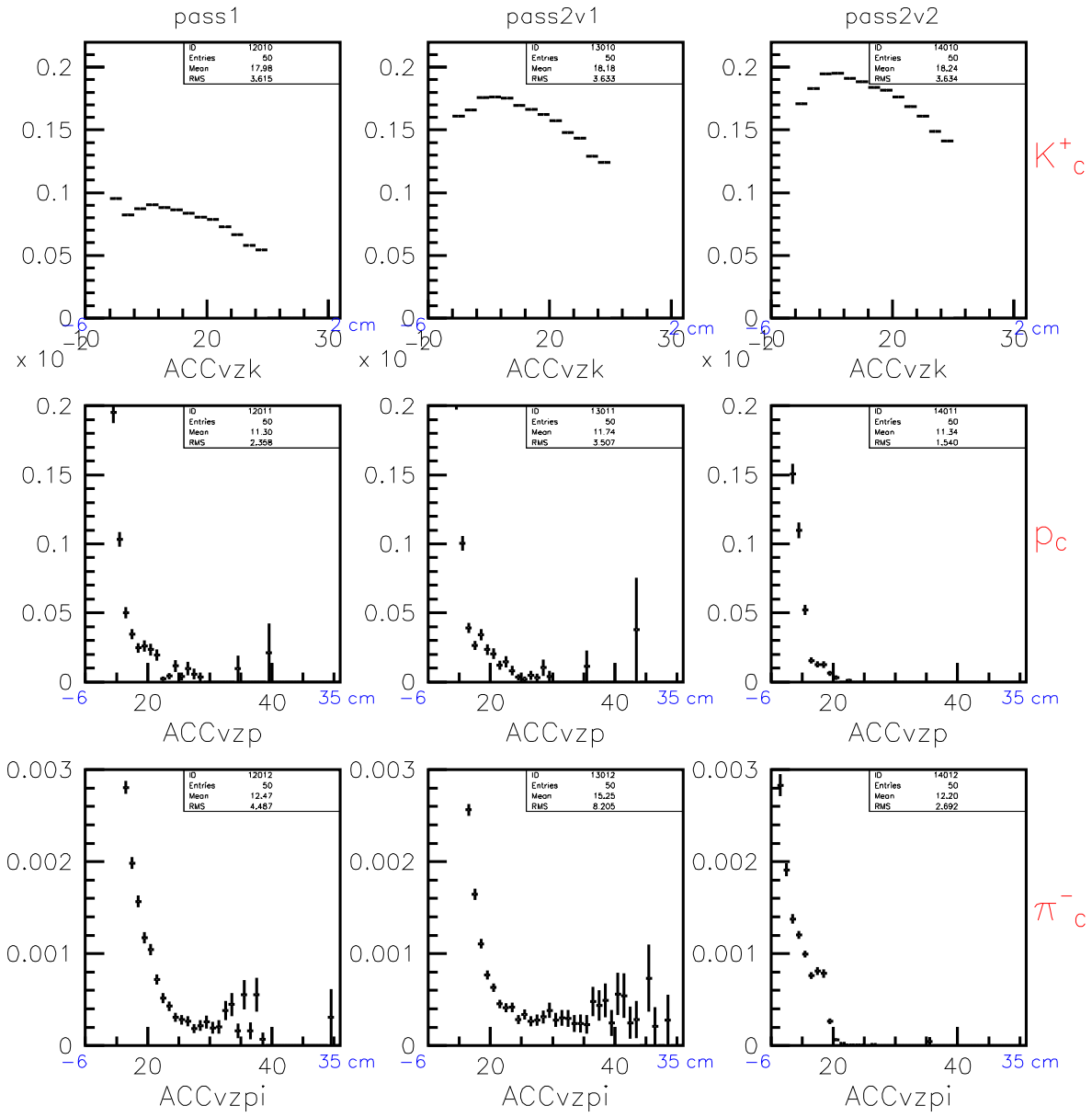

Figure 14: Hadron acceptance vs. z_v from the RG-K $K^+\Lambda$ Monte Carlo (with background) for E_b=6.535 GeV (outbending torus polarity) comparing the pass-1 reconstruction results (6.5.6.2) to the pass-2 reconstruction results (pass-2 v1 - 8.3.2, pass-2 v2 8c.3.2). The electron is reconstructed in the ECAL and the hadrons K^+ (top), p (middle), and π^- (bottom) in the CD.

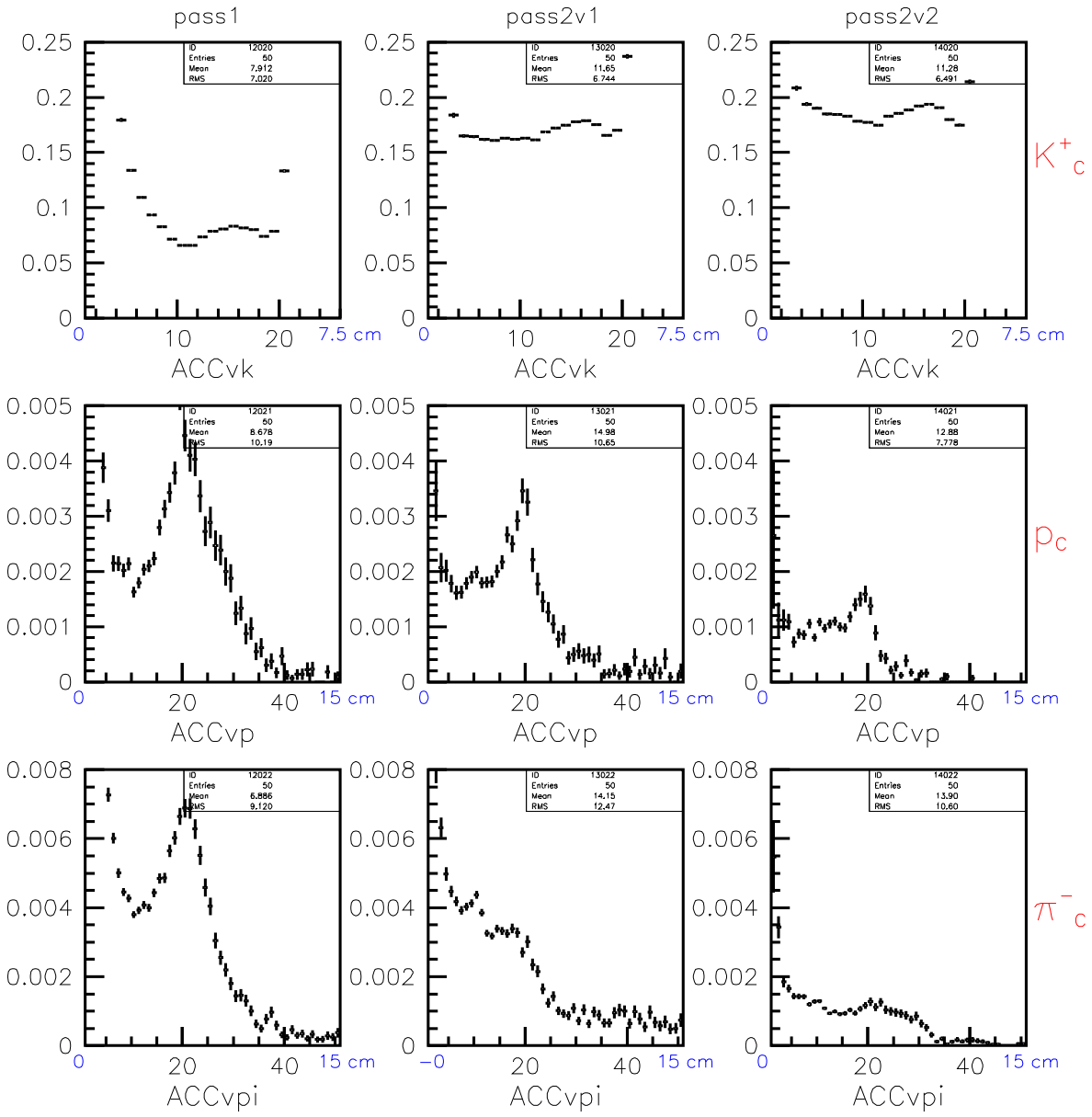

Figure 15: Hadron acceptance vs. vertex position ($\sqrt{x_v^2 + y_v^2 + z_v^2}$) from the RG-K $K^+\Lambda$ Monte Carlo (with background) for E_b=6.535 GeV (outbending torus polarity) comparing the pass-1 reconstruction results (6.5.6.2) to the pass-2 reconstruction results (pass-2 v1 - 8.3.2, pass-2 v2 8c.3.2). The electron is reconstructed in the ECAL and the hadrons K^+ (top), p (middle), and π^- (bottom) in the CD.

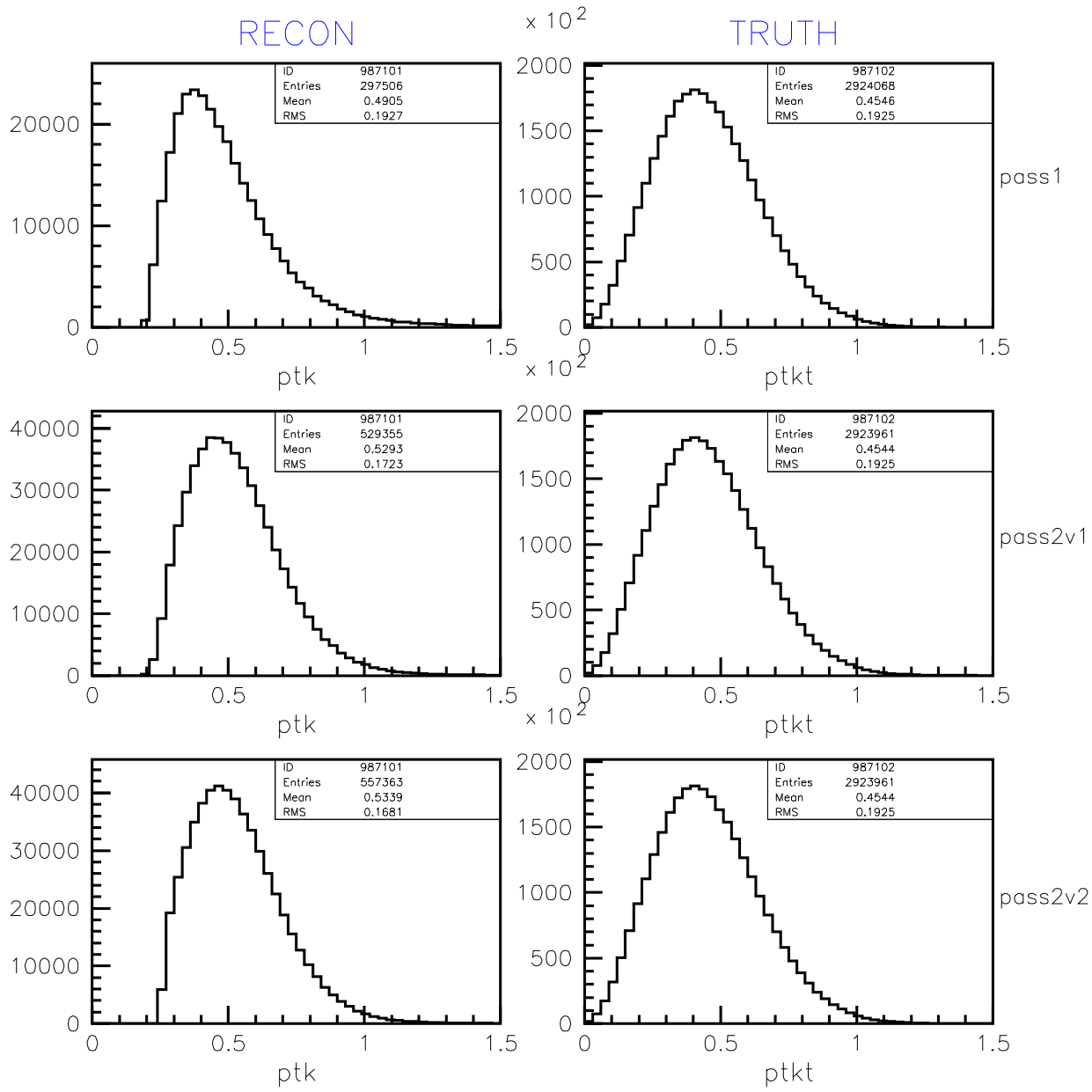

Figure 16: Comparison of reconstructed (left) and generated (right) K^+ transverse momentum distributions from the RG-K $K^+\Lambda$ Monte Carlo (with background) for E_b=6.535 GeV (outbending torus polarity) comparing the pass-1 reconstruction results (6.5.6.2) to the pass-2 reconstruction results (pass-2 v1 - 8.3.2, pass-2 v2 8c.3.2). The electron is reconstructed in the ECAL and the K^+ in the CD.

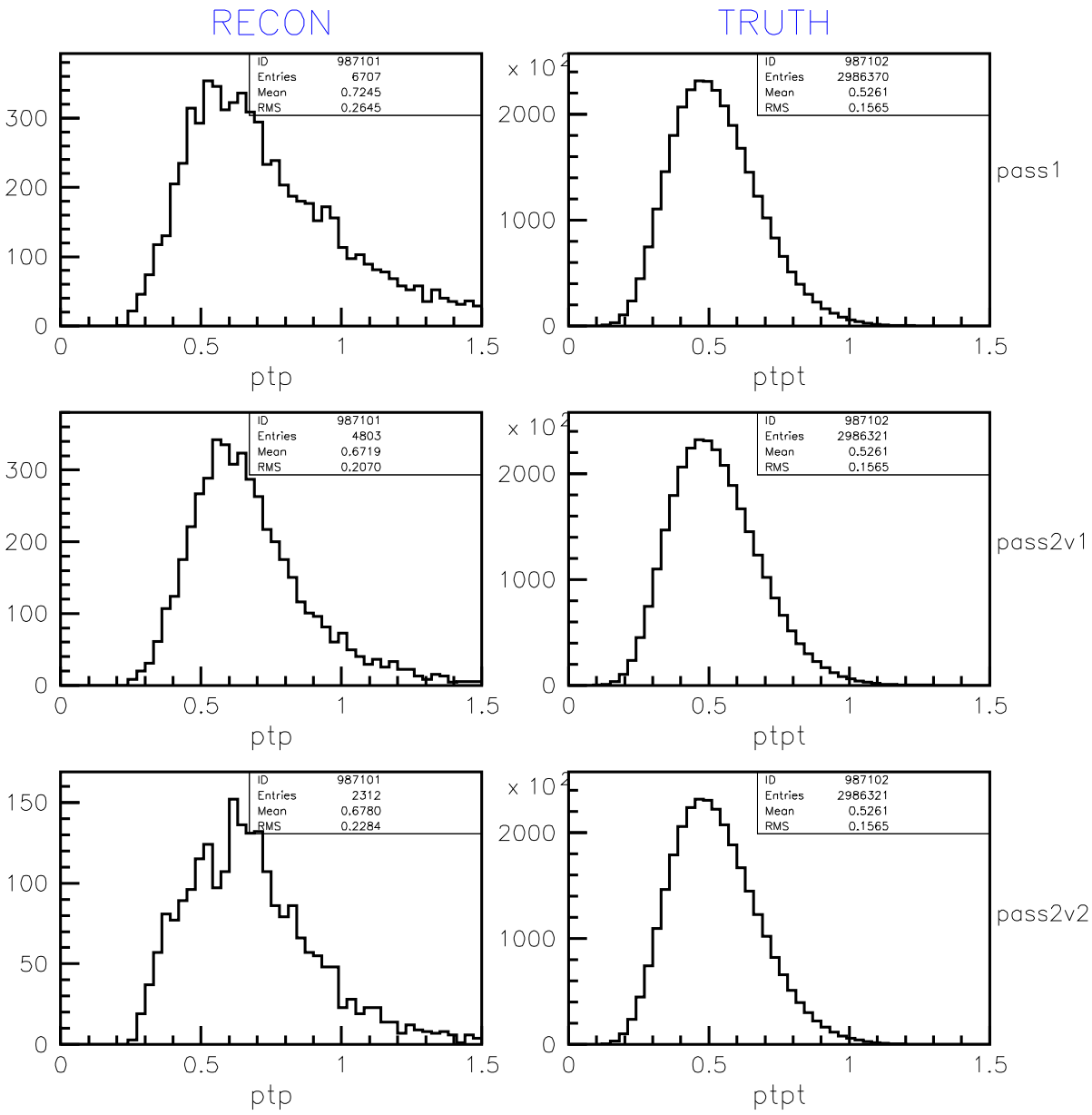

Figure 17: Comparison of reconstructed (left) and generated (right) p transverse momentum distributions from the RG-K $K^+\Lambda$ Monte Carlo (with background) for E_b=6.535 GeV (out-bending torus polarity) comparing the pass-1 reconstruction results (6.5.6.2) to the pass-2 reconstruction results (pass-2 v1 - 8.3.2, pass-2 v2 8c.3.2). The electron is reconstructed in the ECAL and the p in the CD.

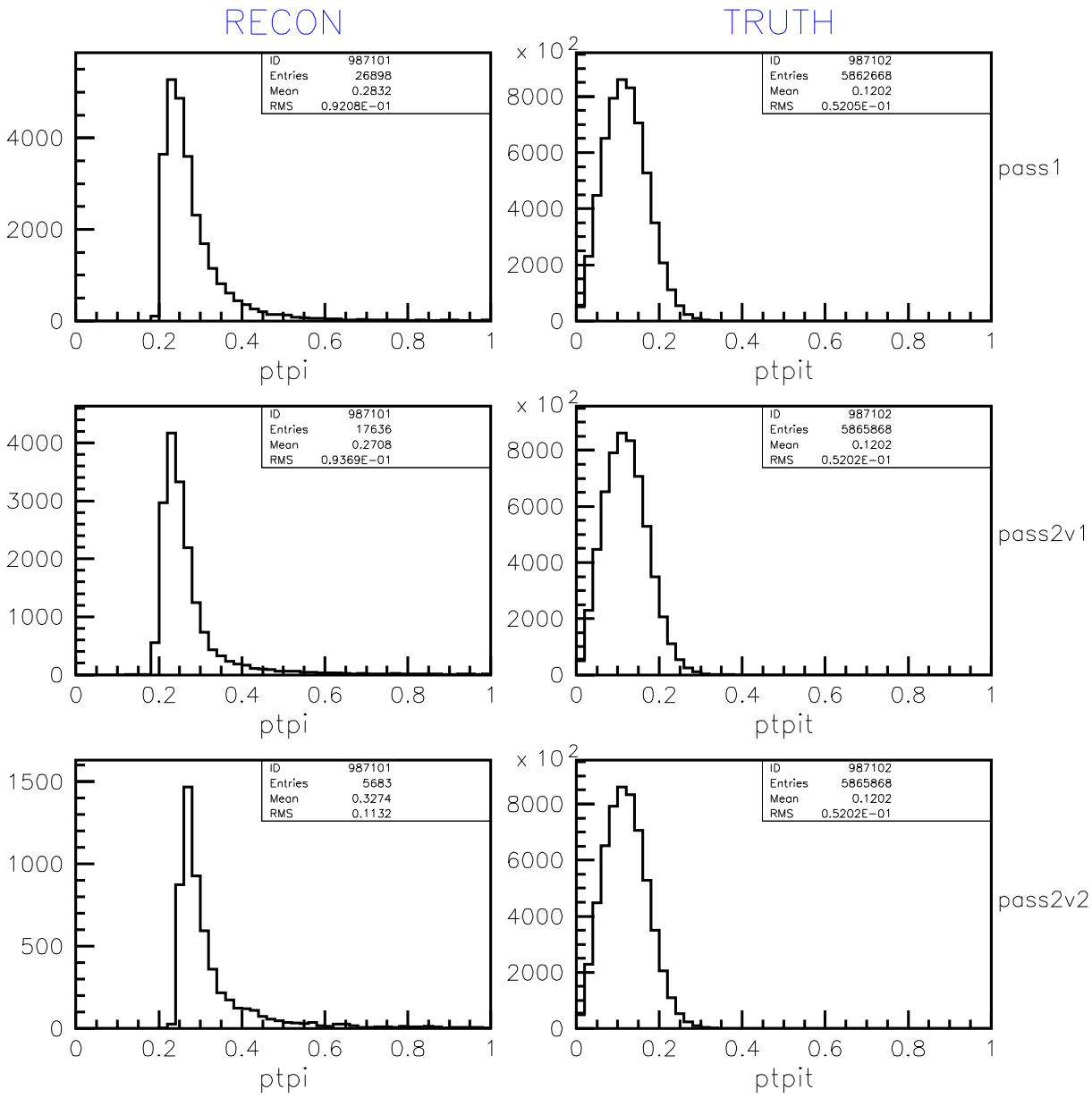

Figure 18: Comparison of reconstructed (left) and generated (right) π^- transverse momentum distributions from the RG-K $K^+\Lambda$ Monte Carlo (with background) for E_b=6.535 GeV (outbending torus polarity) comparing the pass-1 reconstruction results (6.5.6.2) to the pass-2 reconstruction results (pass-2 v1 - 8.3.2, pass-2 v2 8c.3.2). The electron is reconstructed in the ECAL and the π^- in the CD.

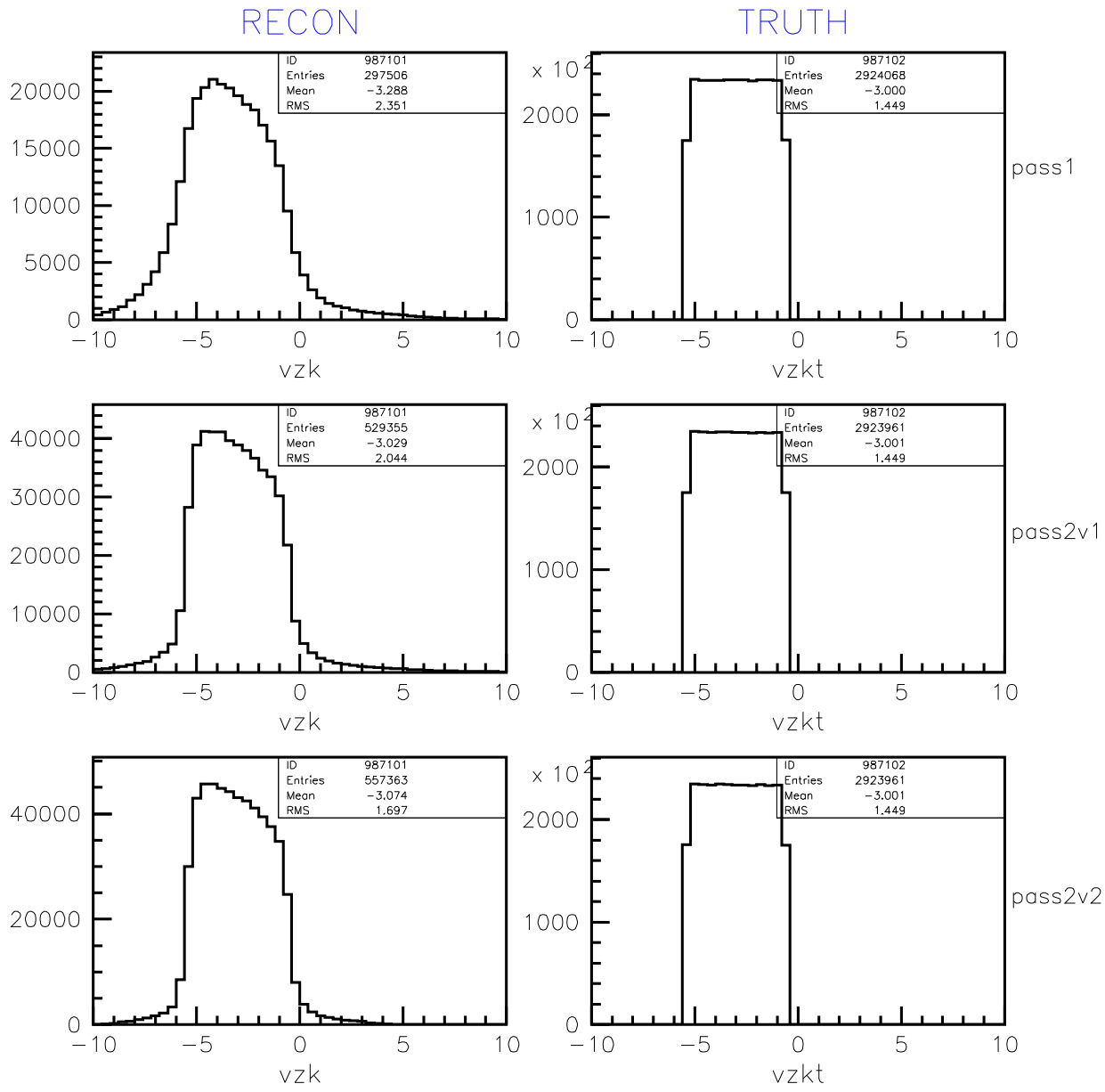

Figure 19: Comparison of reconstructed (left) and generated (right) K^+ z_v distributions from the RG-K $K^+\Lambda$ Monte Carlo (with background) for E_b=6.535 GeV (outbending torus polarity) comparing the pass-1 reconstruction results (6.5.6.2) to the pass-2 reconstruction results (pass-2 v1 - 8.3.2, pass-2 v2 8c.3.2). The electron is reconstructed in the ECAL and the K^+ in the CD.

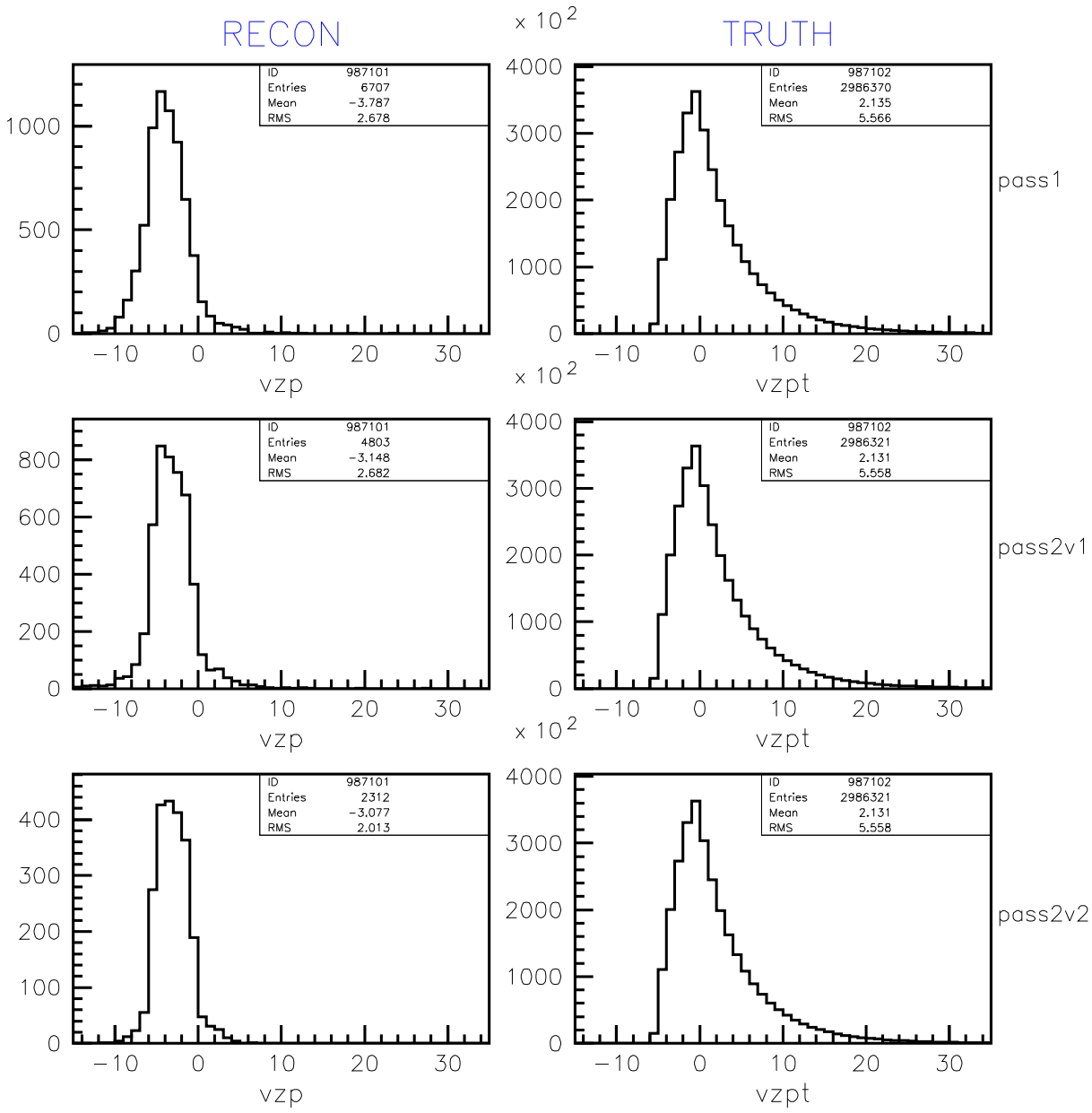

Figure 20: Comparison of reconstructed (left) and generated (right) p z_v distributions from the RG-K $K^+\Lambda$ Monte Carlo (with background) for E_b=6.535 GeV (outbending torus polarity) comparing the pass-1 reconstruction results (6.5.6.2) to the pass-2 reconstruction results (pass-2 v1 - 8.3.2, pass-2 v2 8c.3.2). The electron is reconstructed in the ECAL and the p in the CD.

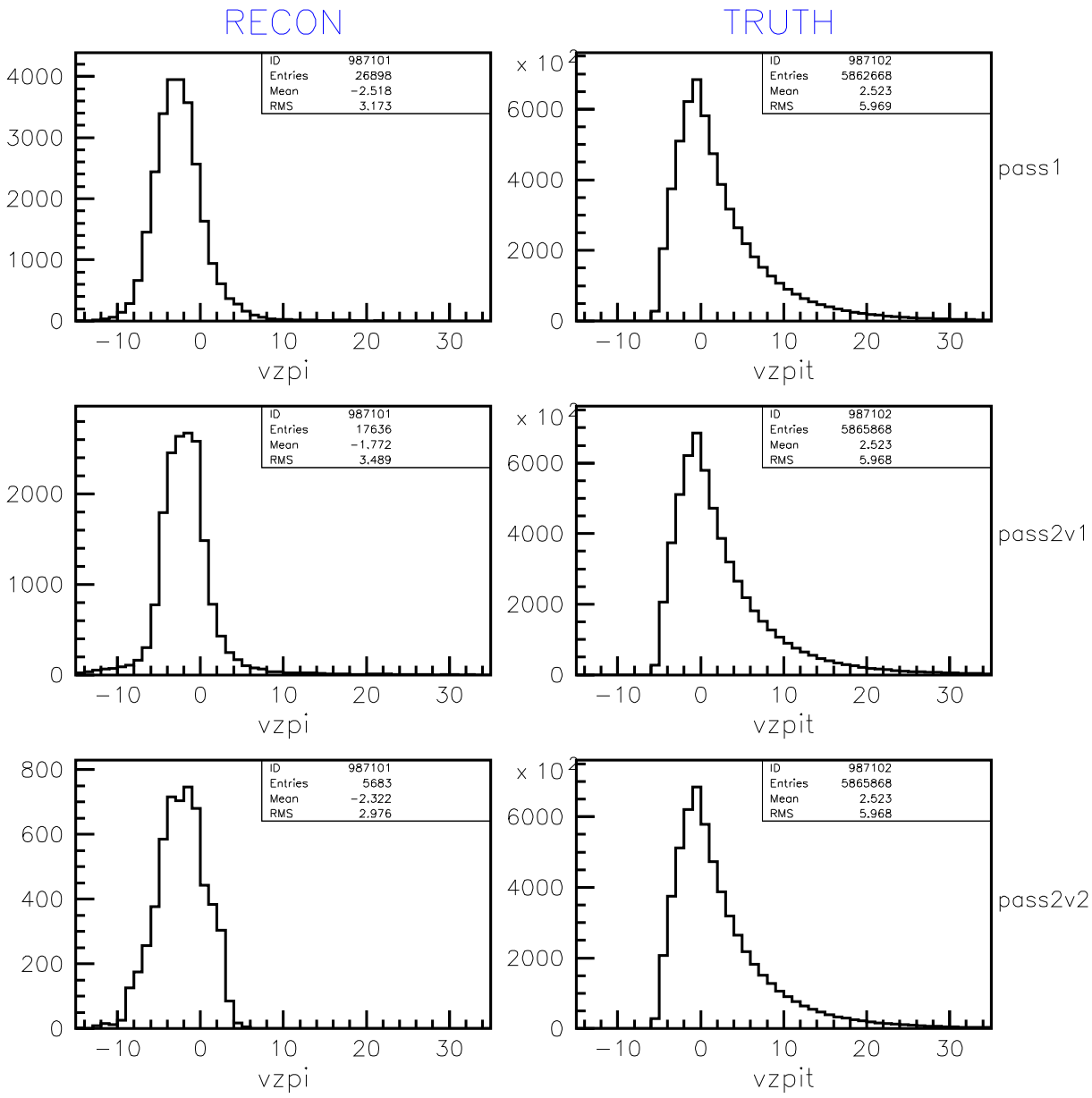

Figure 21: Comparison of reconstructed (left) and generated (right) π^- z_v distributions from the RG-K $K^+\Lambda$ Monte Carlo (with background) for E_b=6.535 GeV (outbending torus polarity) comparing the pass-1 reconstruction results (6.5.6.2) to the pass-2 reconstruction results (pass-2 v1 - 8.3.2, pass-2 v2 8c.3.2). The electron is reconstructed in the ECAL and the π^- in the CD.

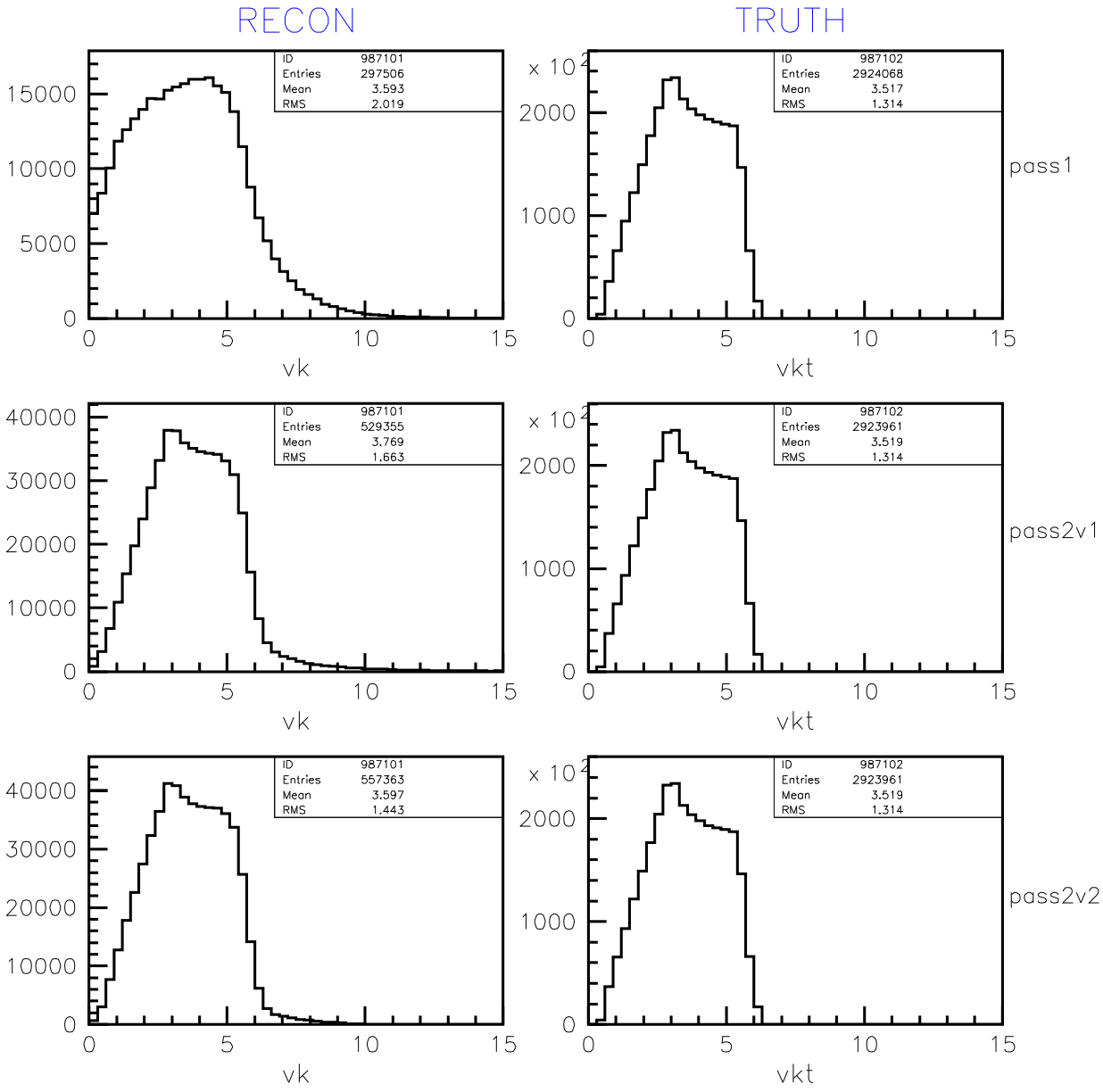

Figure 22: Comparison of reconstructed (left) and generated (right) K^+ vertex position ($\sqrt{x_v^2 + y_v^2 + z_v^2}$) distributions from the RG-K $K^+\Lambda$ Monte Carlo (with background) for E_b=6.535 GeV (outbending torus polarity) comparing the pass-1 reconstruction results (6.5.6.2) to the pass-2 reconstruction results (pass-2 v1 - 8.3.2, pass-2 v2 8c.3.2). The electron is reconstructed in the ECAL and the K^+ in the CD.

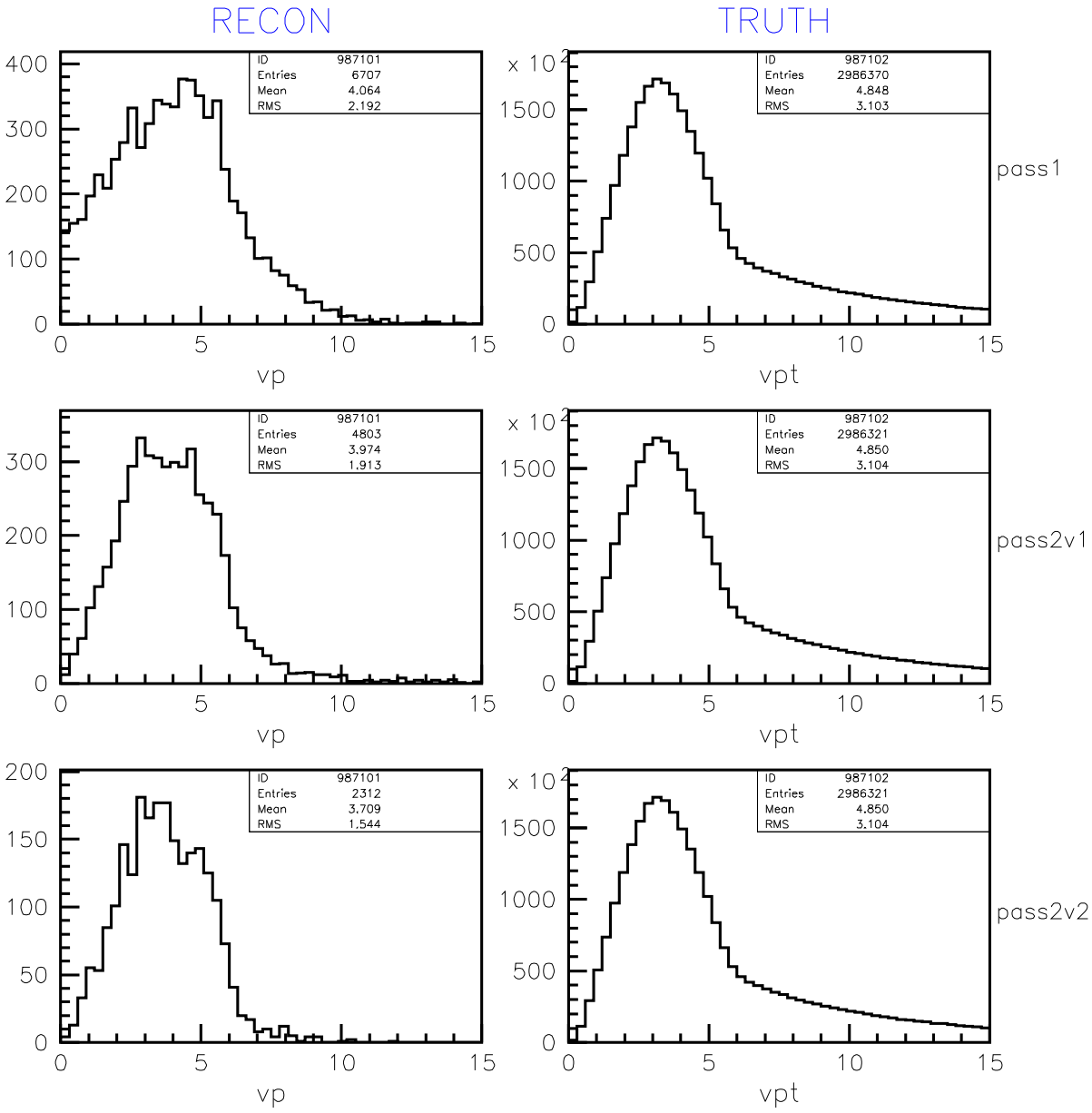

Figure 23: Comparison of reconstructed (left) and generated (right) p vertex position ($\sqrt{x_v^2 + y_v^2 + z_v^2}$) distributions from the RG-K $K^+\Lambda$ Monte Carlo (with background) for E_b=6.535 GeV (outbending torus polarity) comparing the pass-1 reconstruction results (6.5.6.2) to the pass-2 reconstruction results (pass-2 v1 - 8.3.2, pass-2 v2 8c.3.2). The electron is reconstructed in the ECAL and the p in the CD.

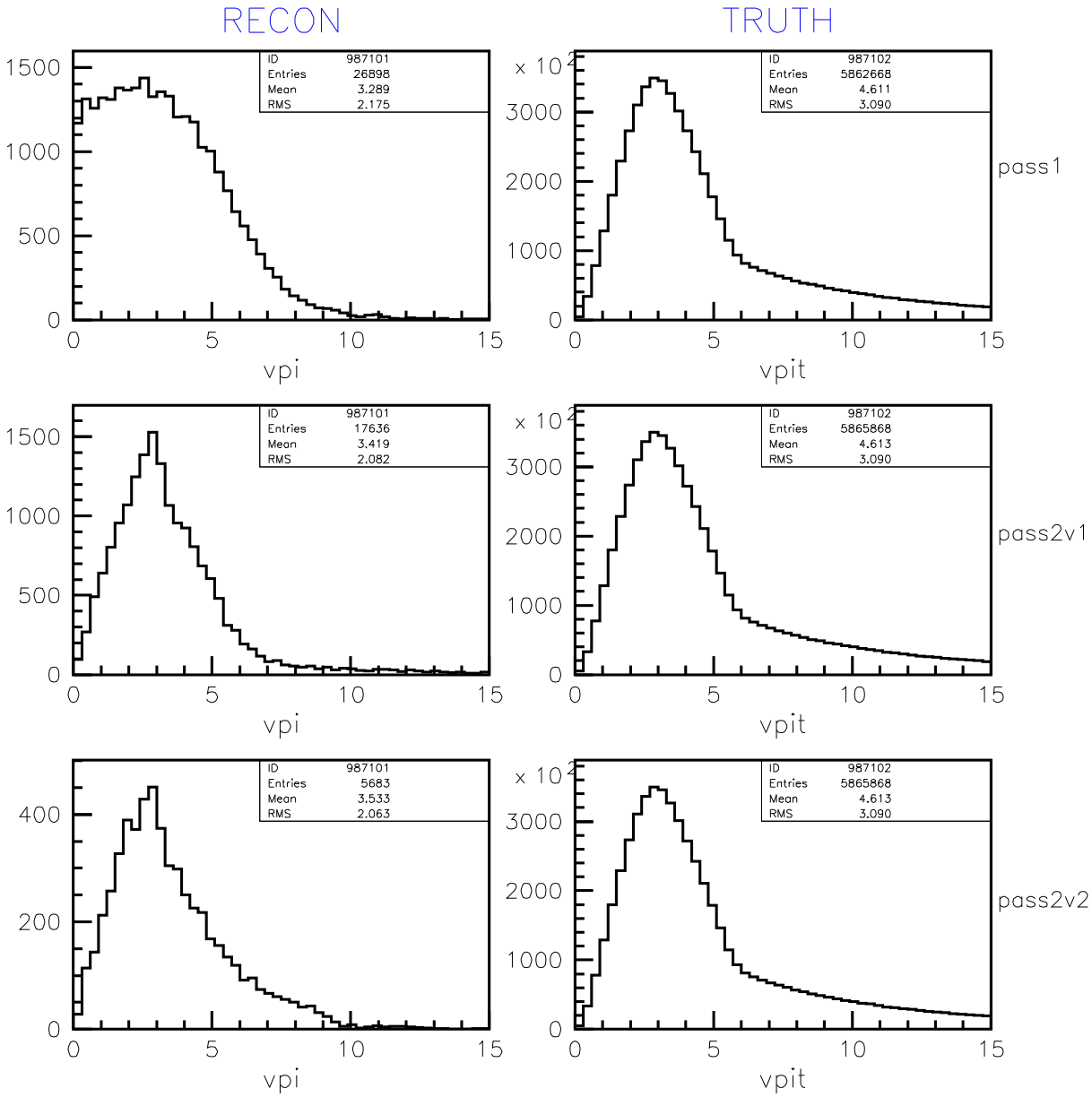

Figure 24: Comparison of reconstructed (left) and generated (right) π^- vertex position ($\sqrt{x_v^2 + y_v^2 + z_v^2}$) distributions from the RG-K $K^+\Lambda$ Monte Carlo (with background) for E_b=6.535 GeV (outbending torus polarity) comparing the pass-1 reconstruction results (6.5.6.2) to the pass-2 reconstruction results (pass-2 v1 - 8.3.2, pass-2 v2 8c.3.2). The electron is reconstructed in the ECAL and the π^- in the CD.

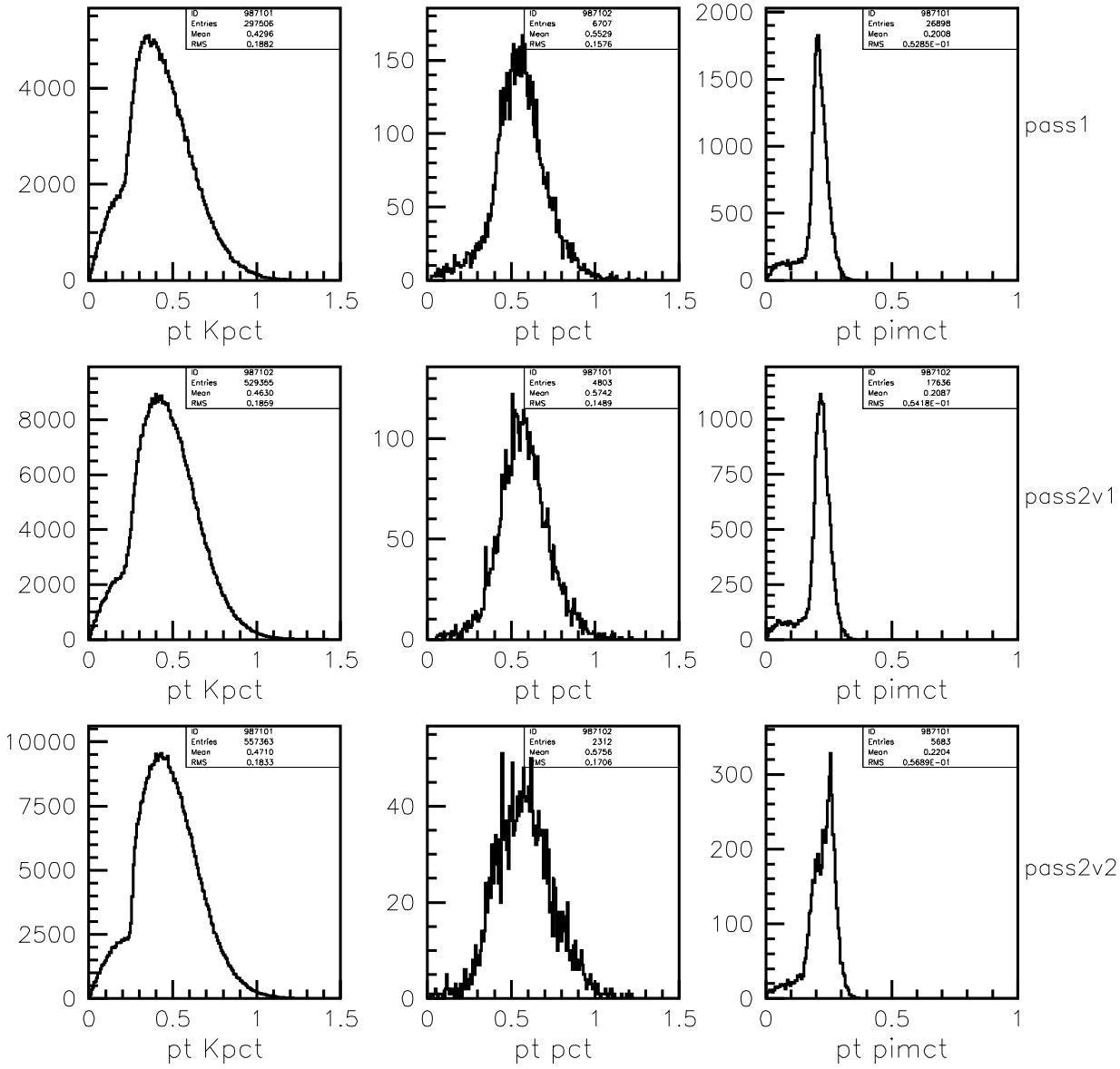

Figure 25: Generated transverse hadron momentum distributions for reconstructed K^+ (left), p (middle), and π^- (right) in the CD from the RG-K $K^+\Lambda$ Monte Carlo (with background) for E_b=6.535 GeV (outbending torus polarity) comparing the pass-1 reconstruction results (6.5.6.2) to the pass-2 reconstruction results (pass-2 v1 - 8.3.2, pass-2 v2 8c.3.2). The electron is reconstructed in the ECAL.

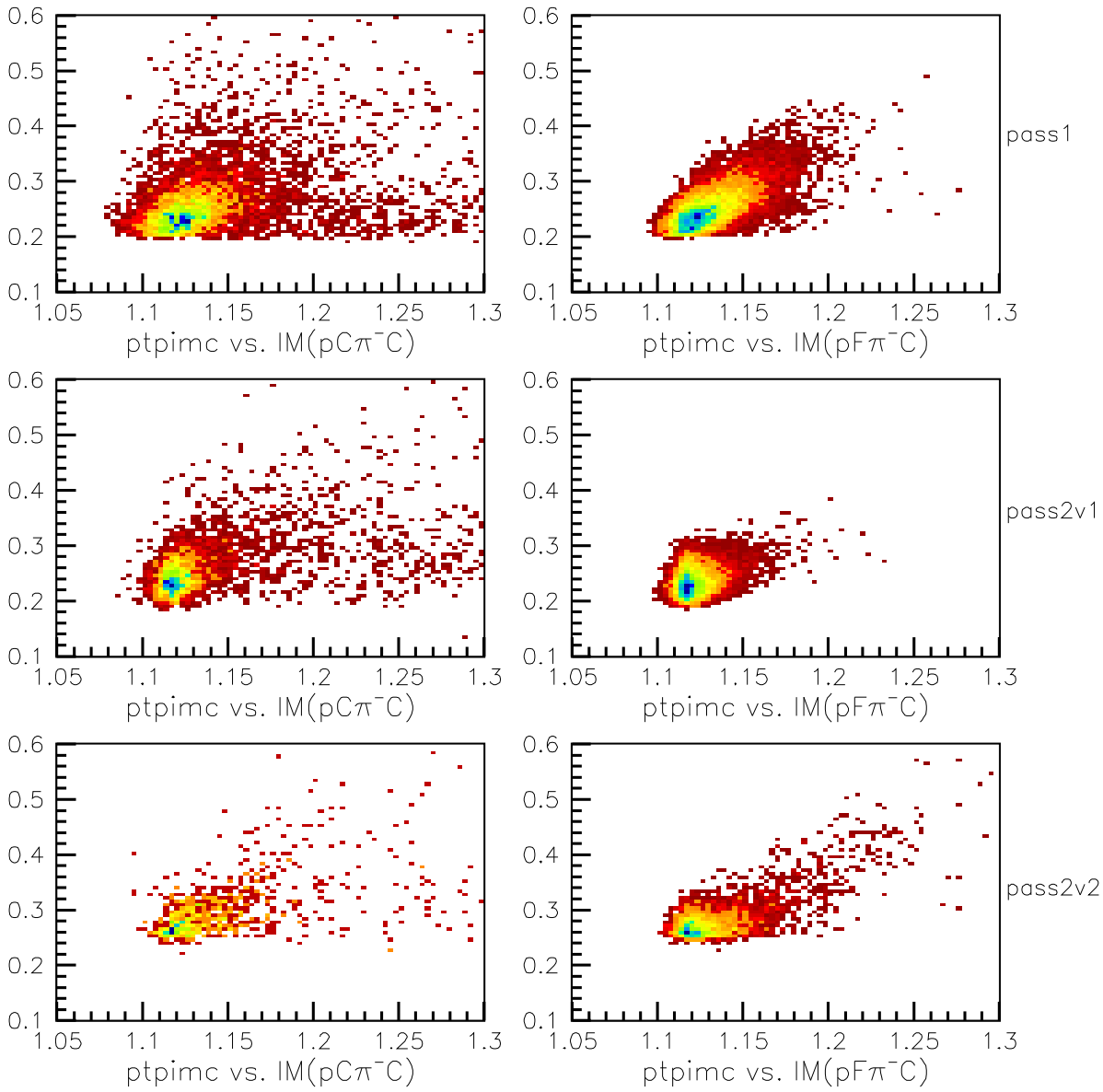

Figure 26: Transverse π^- momentum vs. $M(p\pi^-)$ for π^- in the CD. from the RG-K $K^+\Lambda$ Monte Carlo (with background) for E_b=6.535 GeV (outbending torus polarity) comparing the pass-1 reconstruction results (6.5.6.2) to the pass-2 reconstruction results (pass-2 v1 - 8.3.2, pass-2 v2 8c.3.2). The left column is for the topology with the p in the CD and the right column is for the topology with the p in the FD. The electron is reconstructed in the ECAL.

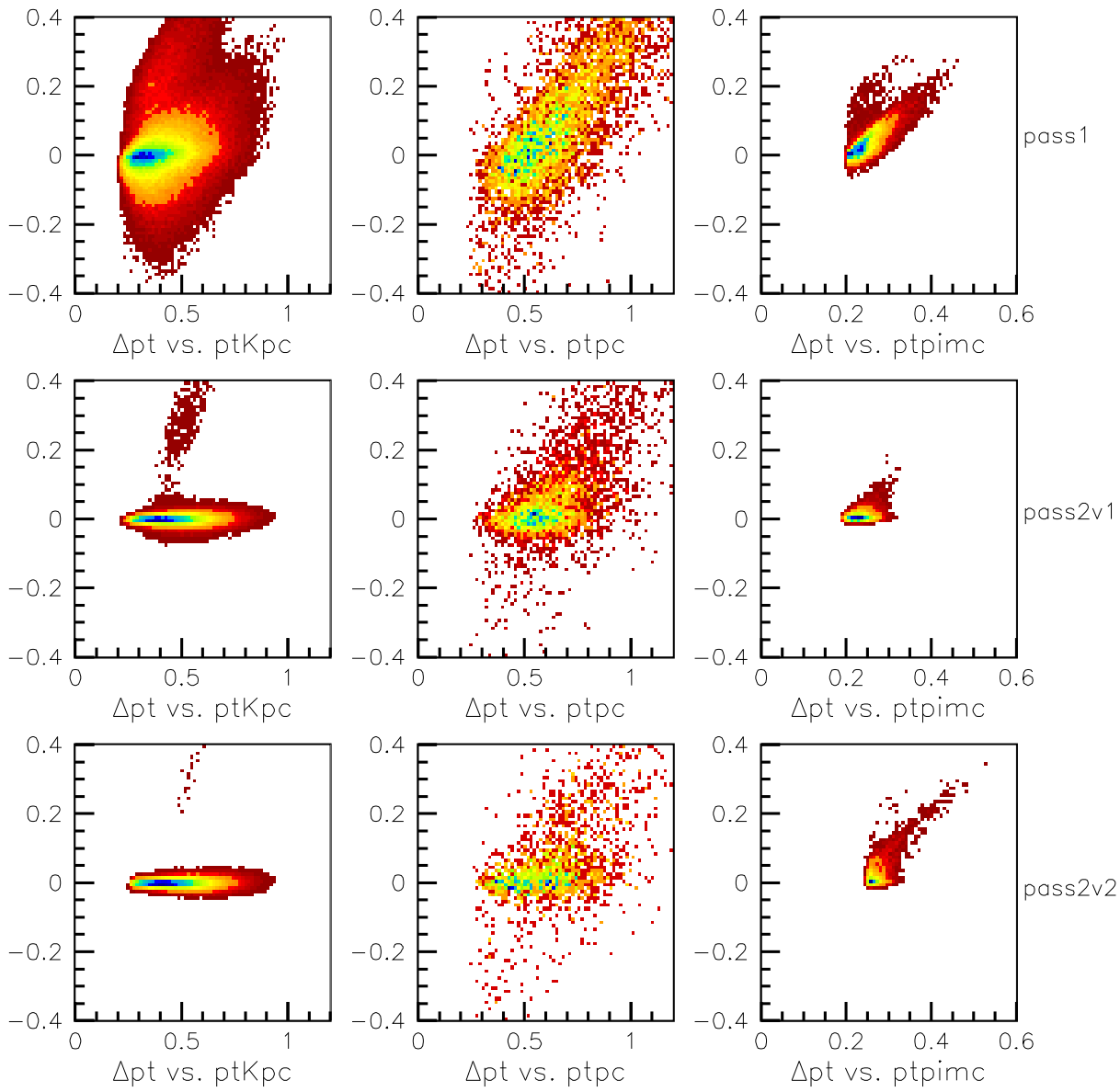

Figure 27: Transverse hadron momentum difference ($p_T^{recon} - p_T^{truth}$) for K^+ (left), p (middle), and π^- (right) in the CD vs. transverse hadron momentum from the RG-K $K^+\Lambda$ Monte Carlo (with background) for E_b=6.535 GeV (outbending torus polarity) comparing the pass-1 reconstruction results (6.5.6.2) to the pass-2 reconstruction results (pass-2 v1 - 8.3.2, pass-2 v2 8c.3.2). The electron is reconstructed in the ECAL.

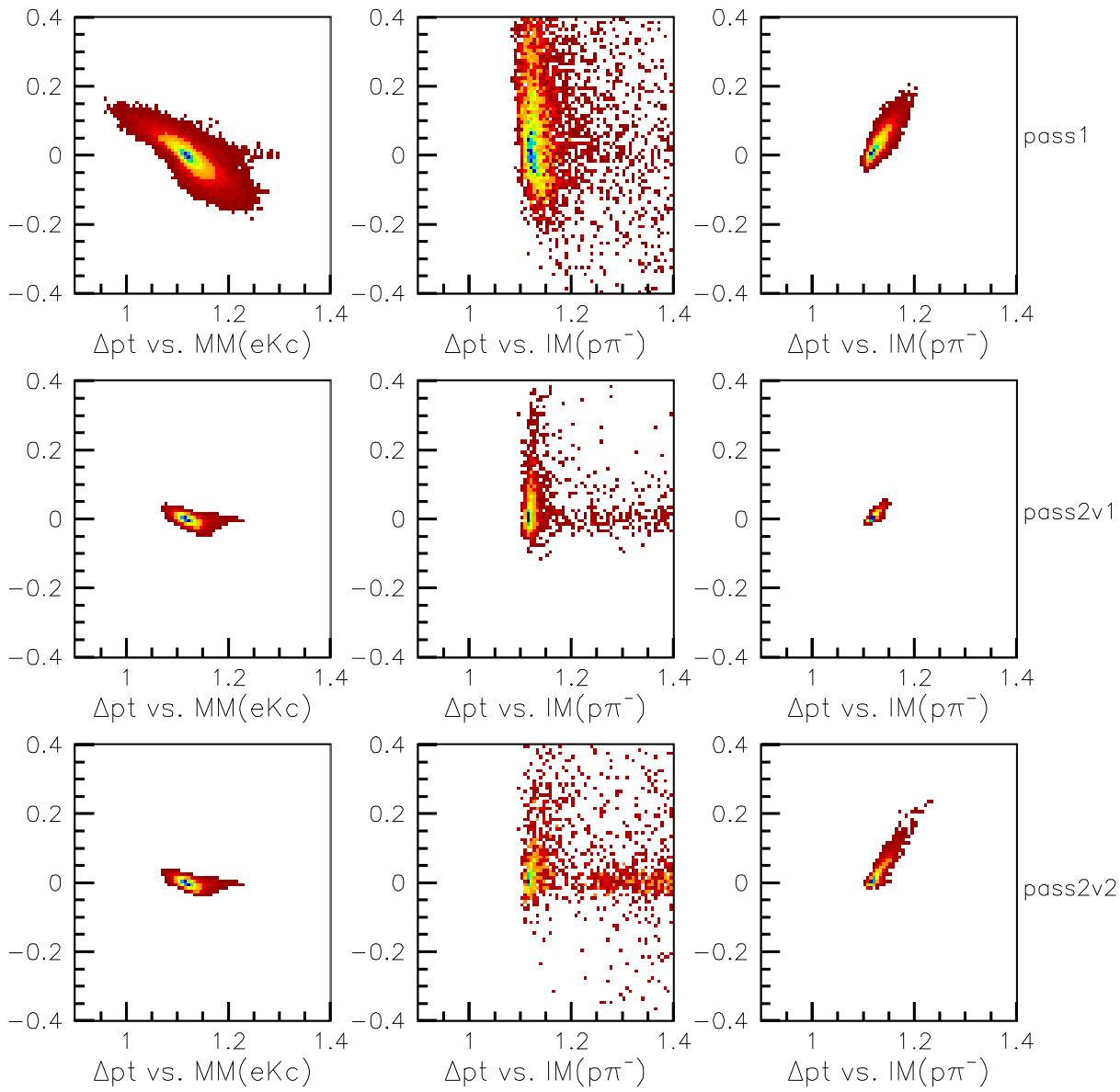

Figure 28: Transverse hadron momentum difference ($p_T^{recon} - p_T^{truth}$) for K^+ (left), p (middle), and π^- (right) in the CD vs. $MM(e'K_C^+)$ (left), $IM(p_C\pi^-)$, and $IM(p\pi_C^-)$ (right) from the RG-K $K^+\Lambda$ Monte Carlo (with background) for E_b=6.535 GeV (outbending torus polarity) comparing the pass-1 reconstruction results (6.5.6.2) to the pass-2 reconstruction results (pass-2 v1 - 8.3.2, pass-2 v2 8c.3.2). The electron is reconstructed in the ECAL.

- genKYandOnePion Event Generator:
  - $ep \rightarrow e'K^+\Lambda$, $\Lambda \rightarrow p\pi^-$ (with proper $c\tau$)
  - Q^2: 0.2 - 5.5 GeV, W: 1.55 - 3.3 GeV, z_v: -5.5 - 0.5 GeV
- Analysis:
  - EB PID
  - chi2pid < 8 (e', hadrons), p_{min}=100 MeV (CD), p_{max}=300 MeV
  - β_{FD}: 0.4 - 1.1, β_{CD}: 0.2 - 1.1
- pass-1 - 6.5.6.2: No cuts
- pass-2 v1 - 8.3.2: p_T^{min}=125 MeV, z_v <30 cm
- pass-2 v2 - 8c.3.2: p_T^{min}=250 MeV, z_v <1 cm